

Lawrence Berkeley National Laboratory

Recent Work

Title

Experimental Evolution of Extreme Resistance to Ionizing Radiation in Escherichia coli after 50 Cycles of Selection.

Permalink

<https://escholarship.org/uc/item/0mt359p5>

Journal

Journal of bacteriology, 201(8)

ISSN

0021-9193

Authors

Bruckbauer, Steven T
Trimarco, Joseph D
Martin, Joel
et al.

Publication Date

2019-04-01

DOI

10.1128/jb.00784-18

Peer reviewed

Experimental evolution of extreme resistance to ionizing radiation in *Escherichia coli* after 50 cycles of selection

Running title: Directed Evolution of Resistance to Ionizing Radiation

Steven T. Bruckbauer¹, Joseph D. Trimarco^{1,2}, Joel Martin³, Brian Bushnell³, Katherine A. Senn⁴, Wendy Schackwitz³, Anna Lipzen³, Matthew Blow³, Elizabeth A. Wood¹, Wesley S. Culbertson^{5,6}, Christa Pennacchio³, and Michael M. Cox^{1#}

¹ Department of Biochemistry, University of Wisconsin – Madison. Madison, WI 53706-1544,

² Present address: Duke Microbiology and Molecular Genetics, Duke University School of Medicine. Durham, NC 27710,

³ DOE Joint Genome Institute - 2800 Mitchell Drive Walnut Creek, CA 94598,

⁴ Department of Biomolecular Chemistry, University of Wisconsin – Madison. Madison, WI 53706-1544,

⁵ Department of Medical Physics, School of Medicine and Public Health, University of Wisconsin – Madison. Madison, WI 53705-2275,

⁶ Department of Medical Physics, University of Wisconsin – Madison. Madison, WI 53705-2275.

#Corresponding author: E-mail: cox@biochem.wisc.edu

Abstract

In previous work (1, 2), we demonstrated that *Escherichia coli* could acquire substantial levels of resistance to ionizing radiation (IR) via directed evolution. Major phenotypic contributions involved adaptation of organic systems for DNA repair. We have now undertaken an extended effort to generate *Escherichia coli* populations that are as resistant to IR as *Deinococcus radiodurans*. After an initial 50 cycles of selection using high-energy electron beam IR, four replicate populations exhibit major increases in IR resistance, but have not yet reached IR resistance equivalent to *D. radiodurans*. Regular deep sequencing reveals complex evolutionary patterns with abundant clonal interference. Prominent IR resistance mechanisms involve novel adaptations to DNA repair systems, and alterations in RNA polymerase. Adaptation is highly specialized to resist IR exposure, as isolates from the evolved populations exhibit highly variable patterns of resistance to other forms of DNA damage. Sequenced isolates from the populations possess between 184 and 280 mutations. IR resistance in one isolate, IR9-50-1, is derived largely from four novel mutations affecting DNA and RNA metabolism: RecD A90E, RecN K429Q, and RpoB S72N/RpoC K1172I. Additional mechanisms of IR resistance are evident.

Importance

Some bacterial species exhibit astonishing resistance to ionizing radiation, with *Deinococcus radiodurans* being the archetype. As natural IR sources rarely exceed mGy levels, the capacity of *Deinococcus* to survive 5,000 Gy has been attributed to desiccation resistance. To understand the molecular basis of true extreme IR resistance, we are using experimental evolution to generate strains of *Escherichia coli* with IR resistance levels comparable to *Deinococcus*. Experimental evolution has previously generated moderate radioresistance for multiple bacterial species.

However, these efforts could not take advantage of modern genomic sequencing technologies. In this report, we examine four replicate bacterial populations after 50 selection cycles. Genomic sequencing allows us to follow the genesis of mutations in populations throughout selection. Novel mutations affecting genes encoding DNA repair proteins and RNA polymerase enhance radioresistance. However, more contributors are apparent.

Introduction

Ionizing radiation (IR) can damage any cellular component, either through direct ionization by high energy photons and electrons, or indirect ionization from reactive oxygen species (ROS) produced by radiolysis of water molecules. Fortunately, levels of IR sufficient to cause widespread oxidation of proteins or extensive DNA damage (including double strand breaks) are rarely encountered in the environment. Surprisingly, a number of microbial species and a few multicellular organisms have evolved extreme resistance to IR (3, 4). The bacterium *Deinococcus radiodurans* is the first-discovered and remains the best-studied example of this extremophile phenotype. *D. radiodurans* survives exposure to 5,000 Gray (Gy) of IR with no lethality, 1000-times the lethal dose for a human. In the case of this bacterium, extreme IR resistance appears to be a byproduct of natural selection for desiccation tolerance (5-7). *D. radiodurans* is not alone. Organisms with high levels of IR resistance can be found readily, particularly in arid environments (8, 9).

IR resistance in *D. radiodurans* has been attributed in large measure to an enhanced capacity to ameliorate ROS produced by IR using a variety small molecules and metabolites (10-12). *D. radiodurans* possesses a fairly standard complement of DNA repair systems. However, specialized adaptations of those systems and the evolution of a few novel DNA metabolic

functions may contribute substantially to the extraordinary capacity of *D. radiodurans* to repair an extensively damaged genome (13-15).

Substantial increases to bacterial IR resistance can be generated in the laboratory by directed evolution (16-19). The advent of advanced DNA sequencing technologies that reveal genomic changes in populations has revolutionized studies of molecular evolution. Mutational trajectories associated with adaptation have been defined in bacteria (20-26), viruses (27-31), yeast (32, 33), and mammalian tumors (34-45). These studies have greatly enhanced the experimental foundation of many phenomena predicted by evolutionary biology, including clonal interference (22, 24, 33), diminishing returns epistasis (20, 46), and genetic parallelism (21-24, 26, 29).

We have utilized directed evolution as a tool providing a facile path to a better understanding of mechanisms underlying the extreme IR resistance phenotype in bacteria. We previously exposed four replicate populations of *Escherichia coli* to 20 iterative rounds of gamma-ray IR and observed significant increases in IR resistance (1). Focusing on isolates from each population, we determined that IR resistance arose from enhanced DNA repair (reflected in mutant alleles of the recombinase RecA, replicative helicase DnaB, putative helicase YfjK, and replication restart machinery), and changes in the regulation of central metabolism and cellular responses to oxidative damage (through an allele of the anaerobic metabolism transcription factor, FNR) (1, 2, 47).

The overall IR resistance of these populations, while increased substantially, did not reach a level comparable to *D. radiodurans*. Efforts to further enhance the IR resistance phenotype have been constrained both by source decay (altering irradiation dose rate parameters and increasing times required to impose a particular dose on a sample) and by new governmental

policies mandating a general decommissioning of radioactive sources used for research. To generate *D. radiodurans*-like levels of IR resistance in evolved *E. coli*, we have embarked on a new and more ambitious effort with four new populations. This new effort employs a clinical linear accelerator (Linac) of a type utilized for radiation treatment of cancer patients. Using this device to produce a high energy electron beam, we can achieve a dose rate of 72 Gy/min, nearly 4-fold higher than that used in the previous directed evolution study (1, 2). Use of this instrument eliminates the problem of radioactive source decay and greatly reduces the amount of time required for exposure to kGy levels of IR. The higher dose rate also allows us to explore adaptation to a potentially much more challenging IR environment than that utilized in earlier trials. We can also begin to assess the effect of dose rate on an evolution trial.

In this report, we characterize the four new *E. coli* lineages (IR9, IR10, IR11, and IR12) after the first 50 rounds of selection (IR9-50, IR10-50, IR11-50, and IR12-50). The dose required to kill 99% of the cells in each population has increased from approximately 750 Gy to over 2000 Gy. These populations are highly resistant compared to the previously evolved isolates CB2000 and CB3000 (1, 2), which appear to be poorly adapted to the higher dose rates applied with the electron beam IR. Deep genomic sequencing of populations after every other selection cycle allow us to explore the full breadth of mutations and provides a revealing window on the evolution of IR resistance. To unveil IR resistance mechanisms, we focus on the genetic parallelism between the four lineages, as reflected in a representative isolate from population IR9-50, IR9-50-1. The results both reinforce some earlier conclusions and offer new insights. The phenotype in IR9-50-1 is largely explained by four mutations, none of which appeared in our previously evolved *E. coli* populations. Although adaptations in DNA repair machinery are again prominent, but now feature novel mutations in *recD* and *recN* which enhance IR

resistance. Furthermore, alterations in RNA polymerase (primarily variants in genes *rpoB* and *rpoC*) also contribute substantially to an IR resistant phenotype. The other three evolved populations exhibit patterns that both reinforce those seen in IR9-50 but also suggest direct competition of two distinct pathways of evolved IR resistance (through either paired mutations of the *recA* and *recD* genes, or a grouping of *rpoB/C*, *recD*, and *recN*). Further adaptation to IR (beyond the mutations described herein) has occurred in each of the four populations, and remains to be explored.

Results

High-energy electron beam IR kills *E. coli* at a similar rate to high-energy photon IR

In this new set of evolution trials, we utilized a Linac to deliver doses with a high energy electron beam. Our previous evolution trials to generate IR resistant *E. coli* utilized a ⁶⁰Co source with a dose rate of approximately 19 Gy/min (1). Using the Linac in electron mode, we were able to deliver the same doses at 72 Gy/min. As there is no source decay with this device, the dose rate will remain constant over the years required for an extended evolution trial. The dose delivered by the Linac was verified using thermoluminescent dosimeters (TLDs). The delivered dose varied by less than 5% of the calculated dose (Table S1).

Although the Linac electron beam and photon sources are different, the dose delivery mechanisms are very similar. In order to rule out any differences between electron and photon modes, we sought to determine if high-energy electron beam ionizing radiation (IR) kills *E. coli* similarly to high-energy photon IR. We note that the ⁶⁰Co and ¹³⁷Cs sources used in our previous directed evolution studies (1, 2, 47) produced high-energy photons. The Linac used in this study has both an electron and photon mode. By changing the distance of the *E. coli* cultures to the

source of the IR beam, the Gray per minute (Gy/min) dose rate can be made equivalent between these modes. At a dose rate of 17 Gy/min, high energy electrons and photons killed nearly an identical percentage of *E. coli* MG1655 culture at 1000 Gy, with the electron beam being slightly more potent (Fig. 1). Therefore, the two IR modes appear to have comparable effects at the level of bacterial survival.

Directed evolution of extreme IR resistance over 50 rounds of selection

Beginning with a single culture of the *E. coli* strain MG1655 split into four, we generated four IR resistant populations using a modified version of a previously established directed evolution protocol (1) as described in the Materials and Methods and depicted in Fig. 2A.

Using this protocol, we carried out 50 iterative cycles (with selection cycles occurring approximately once per week). The resulting populations were designated IR9-50, IR10-50, IR11-50, and IR12-50 (Fig. 2B). Over these rounds of evolution, the dose required to kill 99% of each culture increased from approximately 750 to 2300 – 2500 Gy (Fig. 3A). At round 50, these populations were highly radioresistant compared to the parent MG1655 strain (Fig. 3B). Previously described IR resistant *E. coli* isolates (1, 2, 47), which were evolved to withstand ⁶⁰Co IR at about 4-fold lower dose rates, were only moderately more resistant to the beam generated by the Linac compared to the parent strain and were greatly surpassed by the populations generated in this study (Fig. 3B). Populations IR9-50, IR10-50, IR11-50, and IR12-50 have not yet reached the level of IR resistance of the bacterium *Deinococcus radiodurans* but have made significant progress towards this goal. We note that *D. radiodurans* was significantly more sensitive to the higher dose rate in the Linac electron source than it was to the lower dose rates in the ⁶⁰Co photon source (Fig. 3B) (4, 11, 13).

Growth phenotypes of evolved population isolates

The IR resistance phenotype of these experimentally-evolved populations was not accompanied by an apparent growth defect in LB rich medium. An isolate from each population at round 50 of selection (IR9-50-1, IR10-50-1, IR11-50-1, and IR12-50-1) produced growth curves comparable to the parent MG1655 strain in LB (Fig. 4A). However, growth defects of these isolates became apparent when inoculated in other growth media. In a defined rich medium supplemented with glucose, EZ medium, isolate IR12-50-1 failed to grow and isolates IR9-50-1 and IR11-50-1 exhibited growth defects easily observed in a standard growth curve (Fig. 4B). The isolate IR10-50-1 grew similarly to MG1655 in EZ medium and was the only of the four isolates to grow in M9 minimal medium supplemented with glucose (Fig. 4C). Although IR9-50-1, IR11-50-1, and IR12-50-1 have potentially inactivating mutations in key amino acid biosynthetic pathways that could prevent growth in minimal medium (IR10-50-1 does not have a mutation which would clearly affect amino acid biosynthesis), supplementing minimal medium with these amino acids did not rescue the ability of these isolates to grow (Fig. S1).

Highly sensitive growth competition assays (48) in LB medium can reveal subtle growth phenotypes of these isolates that are not readily apparent when comparing standard growth curves (Fig. 5). When paired with the parent wild type *E. coli* strain in a mixed culture of LB, all four evolved isolates were rapidly outcompeted, even with significant dilutions to bias the starting culture ratios towards the evolved strains. These results indicated that 50 rounds of selection in this directed evolution protocol came with an underlying fitness cost, even when selection is not being applied.

Evolved isolates exhibit variable resistance to non-IR DNA damaging agents

Isolates from the four evolved populations after 50 cycles of selection revealed that resistance to IR does not correlate in any predictable way with resistance to other DNA damaging agents, even within a single population (Fig. 6 and 7). Multiple isolates from each population exhibited highly variable levels of resistance to UV radiation (Fig. 6), mitomycin C (which causes DNA intrastrand crosslinks), ciprofloxacin (which causes DNA double-strand breaks through inhibition of DNA gyrase), bleomycin (which causes DNA double-strand breaks and apurinic/apyrimidinic sites through a ROS mediated mechanism (49, 50)), and hydroxyurea (which has a complex mechanism of action that both reduces dNTP production and causes ROS-mediated DNA damage) (51-54)(Fig. 7). While some isolates exhibited increased resistance to these DNA-damaging agents, others showed no change or increased sensitivity. The results indicate that the directed evolution trials are generating specialists that are uniquely adapted to IR resistance.

Deep-sequencing reveals unique evolutionary histories of the evolved populations

We utilized deep-sequencing technology to monitor genomic changes as IR resistance increased with continued selection cycles. At every other round of selection, genomic DNA was prepared from each population and submitted to the Joint Genome Institute (Walnut Creek, CA) for sequencing to determine all mutations present in each population. Stitching together these snapshots revealed the underlying complexity of these evolving populations (Fig. 8A-D). Depicted in Fig. 8 are the allele frequencies of all mutations detected above 2% frequency at each even round of selection for each lineage. Each line represents a single mutation; groups of mutations that rise and fall in frequency together are inferred to be linked within a sub-

population. The number of sub-populations and total number of mutations increased rapidly (Fig. 8E). The steady accumulation of mutations over time suggests that mutator strains have not yet appeared in these populations. The complete dataset upon which Fig. 8 is based is provided in Supplementary Data 1 through 4.

Despite starting from the same parent strain, the evolutionary path of each population was unique. The only event in common to each population was the excision of the e14 prophage, as indicated by four mutations in the *icd* gene in which the prophage is inserted (as depicted by the initial single black line appearing in each population in Fig. 8A-D). When e14 is excised, the *icd* gene is restored to the wild-type sequence. Despite excision of e14 occurring quickly in each population, that excision became fixed in only three of them. In the IR10 lineage, the sub-population that lost the e14 prophage was driven extinct by another sub-population and e14 is retained in population IR10-50.

Each lineage experienced significant clonal interference, as depicted by the numerous competing sub-populations in Fig. 8A-D. Competition of sub-populations within lineages IR11 and IR12 significantly reduced the rate of fixation events in each lineage. In IR11 (Fig. 8C), no mutations were able to fix from approximately round 16 to round 50 of selection due to severe clonal interference. In IR12 (Fig. 8D), no subpopulation was able to sweep to fixation until 30 cycles of selection were completed. Although clonal interference is apparent in lineages IR9 and IR10, its effects are far less severe than in IR11 and IR12. In IR9 (Fig. 8A), no subpopulation was able to fix post-e14 phage excision until approximately round 20. After this event, another subpopulation swept to fixation unimpeded (defined as a continuous, linear rate of increasing allele frequency). A final subpopulation was able to eventually reach 100% frequency, but was in competition with a separate subpopulation for approximately 12 rounds of selection.

Surprisingly, lineage IR10 (Fig. 8B) has approximately 6 distinct subpopulations which swept to fixation, and each was not noticeably affected by intra-population competition. The differing trajectories of evolution in each population may reflect the relative fitness of the mechanisms of IR resistance employed by each eventual successful subpopulation.

At round 50 of selection, there were distinct differences in the amounts and types of mutations between populations. Populations IR9-50 and IR10-50 are the most homogenous, with approximately 16 and 17%, respectively, of the total high confidence (> 2% allele frequency) mutations being fixed (detected at > 99% frequency). In contrast, only 4% and 11% of high confidence mutations in IR11-50 and IR12-50 are fixed, respectively (Table 1). Although IR9-50 and IR10-50 shared a similar percentage of fixed mutations, IR9-50 and IR12-50 had the highest total number of mutations. Each population had a ratio of non-synonymous to synonymous mutations greater than two.

GC to AT and AT to GC transitions were detected in high numbers, agreeing with mutational patterns detected in previously evolved IR-resistant *E. coli* populations (1, 2). Base substitutions are approximately 50% transitions and 50% transversions, whereas *E. coli* exposed to ⁶⁰Co gamma-ray irradiation exhibit transversions at about four times the frequency of transitions (1, 55). In particular, GC to TA transitions appeared at very high levels in each population, indicative of significant template-strand 8-oxodG-mediated mutagenesis (56). These results indicated that the selection utilized in the current study produces a substantially different mutational, and perhaps DNA damage, spectrum relative to the populations evolved to resist ⁶⁰Co-produced IR.

Mutations which enhance IR resistance in isolate IR9-50-1

We have begun characterization of evolved IR resistance after 50 cycles of selection. To define mutations that made significant contributions to the phenotype, we counted on a substantial degree of genetic parallelism (21, 22, 26) between the four populations. We focused on mutations meeting the following criteria: i) the mutations were non-synonymous; ii) mutations occurred in a gene that was mutated in at least two additional populations; iii) mutations in the gene achieved at least 10% abundance at some point during selection in each population in which they appeared; and iv) the mutation remained in the population at round 50 of selection. These criteria narrowed the search to mutations appearing in six genes, including those involved in recombinational DNA repair (*dinI*, *recD*, and *recN*), transcription (*rpoB*), regulation of anaerobic metabolism (*arcB*), and copper ion transport (*copA*). Two additional gene alterations were analyzed: Nth C203Y and RecA A290S. These did not meet the criteria we set in the current study but were the only two variants, aside from the loss of the ϕ 14 prophage, where the exact same mutation appeared in two populations. The RecA A290S variant, which is fixed in population IR10-50 and also appears in the IR11 lineage, is the only variant detected in this current study that was also detected in an earlier study (1). The relevant variants are listed in Table 2.

To determine the molecular basis of IR resistance in one of the populations, we more carefully characterized one isolate from population IR9-50: IR9-50-1. IR9-50-1 contained over 300 mutations (Table 3). A complete dataset for mutations found within the sequenced isolates is presented in Supplementary Data 1 through 5, with isolate data in the appropriate lineage data file.

IR9-50-1 is representative of several mutational patterns seen in most of the populations, as it has mutations in *dinI*, *recD*, *recN*, *rpoB*, *rpoC*, and *copA* (which contain the majority of

mutations listed in Table 2). This isolate does not have mutations in *arcB*, *nth*, and *recA*. However, a mutation in *arcB*, leading to the variant gene product ArcB N405D, did appear earlier in the IR9 lineage but was driven to extinction via clonal interference. As such, five protein variants present in IR9-50-1 were investigated for contributions to IR resistance: RecD A90E, RecN K429Q, DinI R28H, RpoB S72N, and CopA V270F. The ArcB N405D mutation was also examined as it represented a mutational pattern in other populations. A mutation in *rpoC* (which codes for the K1172I variant) was also included in the strains with RpoB S72N, as the genomic proximity of *rpoC* to *rpoB* did not allow for ready separation of these two mutations with the methods used here.

To assess the potential contribution of mutations identified in this way to IR resistance, we first isolated each mutation in an otherwise wild-type genetic background. We then took the evolved isolate and converted the mutation being studied to wild-type in the otherwise mutant background to determine if it caused phenotypic loss. We moved these mutations singly and in combination into a derivative of the parent *E. coli* strain (MG1655) lacking the ϕ 14 prophage (as this prophage appears to excise from the chromosome after IR exposure and each subsequent mutation occurred in this genetic background (1, 2)). This strain, Founder $\Delta\phi$ 14 (1, 2), thus provided the otherwise wild-type genetic background to determine the contribution of each mutation to IR resistance. We determined that the RecD A90E and RpoB S72N/RpoC K1172I variants each provided a significant increase in IR resistance (Fig. 9A) when isolated in this otherwise wild type background. A combination of these two alleles did not significantly increase IR resistance of the parent strain beyond either individual mutation, indicating that they do not contribute additively. The effects of these two alleles were confirmed by converting each of them singly and in combinations to the wild-type allele in the IR9-50-1 genetic background

(Fig. 9B). Interestingly, the RecN K429Q mutation did not significantly alter IR resistance of Founder Δ e14. However, when this variant was converted to the wild-type RecN in the IR9-50-1 genetic background, IR resistance was dramatically lowered. When these four mutations were eliminated from a derivative of IR9-50-1 that retained the other 308 mutations, IR resistance was not reduced lower than the wild-type RecN single mutant, suggesting a key role for the RecN K429Q variant.

The RecD A90E mutation appeared to be at least a partial loss of function, as deleting the *recD* gene from Founder Δ e14 increased IR resistance just as much as the RecD A90E variant (Fig. 9A). These data agree with the fact that a truncated, and likely inactive, RecD variant appeared earlier in the IR9 lineage and in the IR10 lineage (Table 2). The DinI, CopA, and ArcB variants did not contribute significantly to IR resistance when isolated in the wild type background; additionally, converting the *dinI* or *copA* genes to the wild-type sequence in IR9-50-1 did not increase IR sensitivity of this strain.

Following the allele frequency of mutations in genes that demonstrably contributed to IR resistance (*recA*, *recD*, *recN*, and *rpoB*), a new pattern emerged (Fig. 10). In the lineages IR9, IR11, and IR12 there was a conserved temporal order in the appearance of mutations. First, the e14 prophage was lost, followed by an *rpoB* mutation and then a *recD* mutation along with a *recN* mutation. In the IR12 lineage, the primary *rpoB* mutation was a synonymous coding mutation. However, this did not negate a possible effect of this mutation, potentially at the level of codon usage (RpoB D1203, GAC (WT) to GAT (mutant): 0.37 to 0.63 frequency). The trend was clear in lineages IR9 and IR11, where all the mutations were non-synonymous. IR10 was the only lineage that did not conform to this trend. Although the e14 prophage did excise in lineage IR10, the sub-population that lost the prophage was outcompeted by another that maintained the

prophage and contained a variant of both RecD (N124D) and RecA (A290S). This RecA variant, A290S, was previously observed in *E. coli* populations evolved to resist IR (1, 2) and also significantly contributes to electron beam IR resistance (Fig. S2). This is the only mutation observed in these four populations that appeared in the previously evolved *E. coli* populations, aside from loss of the e14 prophage (1, 2). After the appearance of the RecA A290S and RecD N124D variants, no RpoB variants appeared in the IR10 lineage until nearly round 40 of selection, and those variants (F15L and K1200E) had not yet reached even 50% frequency in IR10 at round 50. It appears that the evolutionary path observed in IR10 nearly occurred in population IR12 as well, where the sub-population that lost the e14 prophage was almost outcompeted by a different lineage (the competing sub-population again featuring RecD (T568A) and RecA variants (E19K)), before being carried to fixation with the apparent help of a different RecD variant (S92I). A sub-population with a RecD (W534R) and RecA variant (E286G) also reached high frequency in IR11 but was slowly outcompeted by a subpopulation with a different RecD variant (A550E) after it gained a second RpoB variant (P535L). In all of these populations, after either RpoB/RecD/RecN or RecA/RecD variants fixed, the opposing grouping of mutations did not appear within the given population. These results imply that these two evolutionary pathways confer competing yet overlapping mechanisms of IR resistance.

Prominent mutations can contribute to enhanced growth phenotypes

If variants of proteins such as ArcB, CopA, and DinI do not contribute to IR resistance, do they make some other contribution to fitness that explains their prominence? We have previously observed that high frequency mutations in experimentally evolved populations may contribute to enhanced growth rates, rather than IR resistance (47). Part of the selection protocol

involves an outgrowth step, after irradiation, in which mutants that grow slowly could be lost. Consistently, the ArcB N405D mutation significantly enhanced the growth phenotype of Founder $\Delta e14$ in a growth competition assay relative to the same strain with a wild-type ArcB (Fig. 11). The DinI R28H and the CopA V270F mutations had no measurable effect on growth (Fig. S3). Mutations that enhance the growth phenotype of these populations are likely important, as evidenced by their inability to grow well in media aside from LB (Fig. 6) and their inability to compete with Founder $\Delta e14$ in mixed culture without IR selection (Fig. 5). In effect, certain mutations may arise that compensate for growth defects conferred by mutations that contribute to IR resistance or deleterious, hitchhiking mutations. Founder $\Delta e14$ with the RpoB S72N and RpoC K1172I variants is outcompeted quickly by Founder $\Delta e14$ with wild-type RNA polymerase (Fig. 11). These results indicate that in order to develop high levels of IR resistance, mutations which buffer against deleterious effects on viability must also rise to prominence in these populations. Although not arising in the same genetic background, the growth phenotype of the ArcB N405D variant indicates that these populations have developed variants which can enhance growth to the degree which mutations such as the RpoB S72N/RpoC K1172I variants impede growth.

Discussion

It is clear that latent within the *E. coli* genome is a capacity for resistance to extreme doses of ionizing radiation. After 50 rounds of selection with high-energy electron beam IR, the dose required to kill 99% of each of these four replicate populations increased by over three-fold to approximately 2500 Gy (Fig. 3A). After a dose of 1500 Gy, this translates into an increase in survival of 4-5 orders of magnitude (Fig. 3B). The dose of electron beam IR that these strains

can withstand far exceeds that of previously evolved IR-resistant isolates (1, 2) , at least when the new and higher dose rate is applied. These populations vary in their growth phenotypes (Fig. 3B and 4) and resistance to other forms of DNA damage (Fig. 6 and 7), indicating that they are specialized to withstand high doses of IR.

Most laboratory exercises in experimental evolution have been characterized by a rapid decline in the rate of fitness increase, as fitness approaches some biologically determined optimum for a given agent of selection (22, 57, 58). One key difference between the current experiment and many other long-term directed evolution experiments is that the selection agent here is not a constant. The dose of IR inflicted on the populations increases as resistance levels increase. Increased selection pressure to meet a defined, desired phenotype throughout selection is not a novel protocol (58), yet in our evolution experiment there is no evident deceleration in the rate of fitness gains. Genetic patterns (parallelism) have allowed us to identify some key contributors to the growing IR resistance phenotype. However, the continuing advance of IR resistance and allele diversity in all populations also suggests that the pool of potential adaptive mutations is much greater than that now present in any one population. As selection continues, substantial additional gains in unique pathways may be expected. Ionizing radiation is not only a selection agent, but also a potent mutagen. Although this study was not initiated with the goal of exploring mechanisms of molecular evolution, we anticipate that the datasets provided in Supplemental Data 1 through 4 will be of use to investigators in that field.

Modified DNA repair proteins and RNA polymerase enhance IR resistance

Each population has traversed unique evolutionary paths to reach the same goal (Fig. 8A-D). Despite varied levels of clonal interference in each population, significant genetic parallelism

in these populations allow us to identify at least some of the contributors to extreme IR resistance. In one isolate from population IR9-50, IR9-50-1, mutations in *recD*, *recN*, and *rpoB/rpoC* increase IR resistance of the Founder Δ e14 parent-derivative. However, these variants – singly or together – do not account entirely for the IR resistance phenotype of IR9-50-1 at a dose of 1000 Gy (Fig. 9A and B). None of these genes have been previously implicated as mutational targets contributing to IR resistance (1, 2, 47).

The effects of mutations in these genes reveal complex interactions. When present in an otherwise wild-type background, the mutations in *recD* and *rpoB* exhibit a clear contribution to IR resistance, although results with the *recN* mutation were variable. The *recD* and *rpoB* effects were not additive, and combining them demonstrated diminishing returns epistasis. When the *rpoB* mutation was reverted to wild-type in the IR9-50-1 mutant background, the IR resistance phenotype was reduced little or not at all. However, reverting the *recD* and *recN* mutation to wild-type resulted in a considerable loss of IR resistance. It appears likely that a complete genetic deciphering of the IR resistance of IR9-50-1 and other isolates will require a more systematic consideration of relationships between mutations and genetic backgrounds.

Although additional contributions are clearly present, the alterations in RecD, RecN, and RpoB/RpoC (Fig. 9) provide the clearest evidence for phenotypic contributions in the current work. RecD is part of the RecBCD heterotrimer responsible for preparing ssDNA required for RecA loading, initiating homologous recombination. The RecD A90E variant is likely a loss of function mutation, as a RecD deletion in the Founder Δ e14 background increases IR resistance as much as the A90E variant in this background. RecD inactivation produces a hyper-recombination phenotype (59-62). Increased homologous recombination could be of significant

use to repair highly fragmented DNA post-IR, with approximately 15 DSBs generated at 1000 Gy (3).

RecN is a cohesin-like protein which is involved in RecA-mediated double-strand break repair (63-66). There is little known about the precise function of RecN, though it has been implicated in maintaining proximity of broken dsDNA ends to an active RecA filament. The function of the K429Q variant is unknown, but the K429 residue is positioned in a RecN domain highly conserved among bacteria. The K429Q variant is unlikely to be a loss of function, as *recN* deletion greatly enhances IR sensitivity (2, 67). Further work on these RecN variants may shed new light on the function of the RecN protein.

RpoB and RpoC are the beta and beta-prime subunits of RNA polymerase, respectively. Stringent mutations of RNAP, which mimic the effects of ppGpp binding and therefore the stringent response, are located primarily in RpoB and RpoC (68). Some of these stringent mutants are capable of rescuing UV-sensitivity of *ruvABC* mutants of *E. coli*, potentially due to decreased stability of contacts of RNAP with DNA (69, 70). Similar to these previous observations, the mutations in RpoB that are prevalent in our evolved populations do not locate to a single region of RpoB and therefore may affect DNA interaction throughout the DNA channel formed by RpoB/RpoC. Previously described stringent mutations L571Q and H1244Q mutants (69, 70) affect residues near those affected in the current study. These mutations likely decrease stability of RNAP on DNA and may allow for easier removal of RNAP that has stalled at a DNA lesion. Removal of stalled RNAP may be crucial for efficient DNA repair due to RNAP occluding the lesion from repair machinery or providing a major obstacle to DNA replication (71). Additionally, many stringent mutants of RNAP also confer resistance to the antibiotic Rifampicin. Mutated variants of RNAP at P535 (72) and S574 (73-75) (which have

also been isolated in this study) have previously been isolated using selection for rifampicin resistance. Although these are the first RNA polymerase mutations detected in *E. coli* evolved for IR resistance, similar mutants have been generated during experimental evolution of *E. coli* for trimethoprim and doxycycline resistance (58), heat tolerance (76, 77), growth in nutrient-limited conditions (78, 79), and acid resistance (80, 81). Modifications in RNA polymerase may confer enhanced fitness throughout serial passaging, a common feature of experimental evolution studies. This advantage, combined with a potential ability to enhance DNA repair, may explain the rapid appearance of *rpoB* or *rpoC* alleles in each evolving lineage (except IR10).

Excision of the e14 prophage is induced by selection for IR resistance

The only event common to each of the four populations is the excision of the e14 prophage, which was evident by round two of selection. However, in lineage IR10 the subpopulation that lost e14 was outcompeted and driven extinct by cycle ten. Despite no apparent mutations within e14 that may prevent its excision, the e14 prophage remains within lineage IR10. It is unclear why e14 excision is the first clear event to happen in each population (an event that also occurred early in evolution of our previously evolved gamma-ray IR-resistant *E. coli* populations (1, 2). Excision of the e14 prophage is predicted to be under regulation of the SOS response, this event may simply be an artifact of the *E. coli* DNA damage response (82). However, the e14 genome does encode two potentially lethal cell division inhibitor proteins: a homologue of the lambda phage protein Kil and SfiC. Loss of these proteins may itself be selective pressure. Indeed, loss of the e14 has been previously noted during experimental evolution (83) Interestingly, deletion of the e14 prophage has also been observed to cause

variable resistance to many antimicrobial agents, including increased resistance to hydrogen peroxide (84).

Direct competition between two pathways to IR resistance dictates adaptation

Population sequencing also reveals the underlying competition of lineages within each population. Clonal interference is a hallmark of these populations. While much of this study focuses on the current end-point (each population after 50 cycles of selection), observing evolution over the remaining 49 cycles allows us to understand the genetic context in which new mutations arise and how the successful lineages were able to outcompete other fit, but ultimately unsuccessful, lineages. This competition within populations was almost immediately apparent.

There is an apparent competition between lineages which contain alleles of *rpoB* and those with *recA* alleles. In the current protocol, with its much higher IR dose rate, *recA* alleles are less common than observed in our earlier study, and novel *rpoB*, *recD*, and *recN* alleles predominate. In IR9, a single *recA* variant appeared (Y294C) but only reached approximately 12% frequency in the population before being driven extinct by round 20 of selection. This population successfully lost the e14 prophage and then gained an *rpoB* allele followed by *recD* and *recN* alleles. The appearance of *recD* and *recN* alleles in tandem occurred in three of the four populations, and each contributes similarly to IR-resistance in a wild-type background (Fig. S4). In IR10, the RecA/RecD variant pair appears very early, and rapidly outcompetes the lineage that lost the e14 prophage. After this event, the only mutation that became fixed within the population (of those common to all four populations which we are focusing on) is another RecD variant. RpoB variants do not appear until at least round 40 of selection in IR10, and by round 50, these variants do not yet appear to be on a path to fixation. No high-frequency *recN* allele has

appeared in IR10. The IR11 and IR12 lineages followed a path similar to that taken by IR9. In the IR11 lineage, loss of the e14 prophage and subsequent gain of an *rpoB* allele became fixed. In this genetic background, two separate sub-populations containing RecN/RecD and RecA/RecD variants, respectively, later reached prominence. The RecN/RecD subpopulation gained a variant of RpoB which assisted in driving this sub-population to fixation and the RecA/RecD to extinction. Finally, IR12 almost began on a similar evolutionary trajectory as IR10. A sub-population that lost the e14 prophage and gained an *rpoB* allele (which leads to a synonymous coding mutation) was nearly outcompeted by a RecA/RecD variant sub-population, before a RecN/RecD variant-pair rescued the sub-population that had lost e14. By round 40 of selection, the winning subpopulation reached fixation.

Despite our focus on the genetic parallelism between these four populations, it is evident that each population has begun to develop unique adaptations. Of the total number of fixation events in each lineage (excluding excision of the e14 prophage, IR9: 2; IR10: 5; IR11: 2; IR12: 2) tracking mutations in *rpoB/recA/recD/recN* only fully accounts for such events in IR9 and IR11. In all four lineages, major subpopulations that have arisen after fixation of *rpoB/recA/recD/recN* combinations are completely unaccounted for by the criteria used to identify the mutations tested in this study. While it is clear that e14 excision and competition between RecA/RecD and RpoB/RecD/RecN provides a path to enhanced IR resistance, this appears to be only the first step on a complicated fitness landscape. New methods must be applied to determine the unique paths taken by each of the four lineages.

Source of IR and dose rate alter the molecular basis for experimentally-evolved IR resistance

Populations IR9-50, IR10-50, IR11-50, and IR12-50 provide us with a platform for understanding the molecular fundamentals of extreme IR resistance. These populations have been evolved using a source of IR with a much higher dose rate than that used previously to evolve IR resistance in *E. coli* (72 Gy/min versus 19 Gy/min) (1). Isolates from the prior evolved populations, CB2000 and CB3000 (1, 2) are only moderately more resistant to this form of IR compared to the parent strain. The higher dose rate in the current protocol may account for the relative sensitivity of the strains derived from the earlier evolution trial.

There are distinct differences in the mutations which appear in these populations and those that were previously evolved (1, 2). Only a single mutation previously noted to enhance IR resistance, RecA A290S (1), appears in the four new populations. While enhanced DNA repair is a hallmark of the previously evolved populations and the populations presented here, it appears as though the enhancements are indeed different. In addition, the frequency of transversion mutations detected in the new populations (~50% of all mutations) is far higher than that observed in the earlier studies (~20% of all mutations) (1, 55). This appears to be due to the extreme amount of detected GC to TA transitions, specifically. This transition is a hallmark of A mispairing with template-strand 8-oxodG (56), indicating that DNA damage may be more extreme in cells exposed to electron beam IR. However, the high energy electrons and gamma rays produce similar levels of killing (Fig. 1). A more likely explanation lies with the differences in the dose rate applied. In any case, these new *E. coli* lineages are replete with novel mechanisms of experimentally evolved IR resistance.

We do not yet have experimentally evolved *E. coli* that can match the natural IR resistance of the bacterium *D. radiodurans*. However, selection is continuing.

Materials and methods

Growth conditions and bacterial strains used in this study

Unless otherwise stated, *E. coli* cultures were grown in Luria-Bertani (LB) broth (85) at 37°C with aeration. *E. coli* were plated on 1.5% LB agar medium (85) and incubated at 37°C. Overnight cultures were grown in a volume of 3 mL for 16 to 18 hr. Exponential phase cultures were routinely diluted 1:100 in 10 mL of LB medium in a 50 mL Erlenmeyer flask and were grown at 37°C with shaking at 200 rpm and were harvested at an OD₆₀₀ of 0.2, unless otherwise noted. After growth to an OD₆₀₀ of 0.2, cultures were placed on ice for 10 min to stop growth before being used for assays.

Cultures were plated on tetrazolium agar (TA) for growth competition assays when noted (48, 86). The defined rich medium EZ was mixed per manufacturer's specifications and was supplemented with 0.2% glucose or 0.2% glycerol as indicated (Teknova; Hollister, CA). M9 minimal medium (supplemented with 0.2% glucose) was used when indicated (85).

All strains used for *in vivo* assays in this study are mutants of *E. coli* K-12 derivative MG1655. Genetic manipulations to transfer mutations or delete genes were performed as previously described (87, 88). Strains used in this study are listed in Table 4.

Serial dilutions and CFU/mL determination

All serial dilutions were performed in 1X phosphate-buffered saline (PBS) (for 1 L: 8 g NaCl, 0.2 g KCl, 1.44 g Na₂HPO₄, KH₂PO₄ 0.24 g with 800 mL dH₂O, adjust pH with HCl to 7.4, then add remaining 200 mL dH₂O). Unless otherwise stated, serial dilutions were performed with serial 1:10 dilutions of 100 µL of culture or previous dilution into 900 µL 1X PBS. Before transfer to the next dilution tube, samples were vortexed for 2 seconds and mixed by pipetting to ensure mixing. One-hundred µL of appropriate dilutions were aliquoted onto agar plates of the

appropriate medium and were spread-plated utilizing an ethanol-sterilized, bent glass rod. For spot plating, 10 μ L of each dilution was aliquoted onto agar plates of the appropriate medium and spots were allowed to dry before plates were incubated as in *Growth conditions*.

CFU/mL was calculated using the highest CFU count for each strain assayed that remained between 30 and 300 CFU (ex: 250 CFU on a 10^{-4} dilution plate would be used for calculation over 40 CFU on a 10^{-5} dilution plate).

TLD dose validation

An independent dose verification was performed with thermoluminescent dosimeters (TLDs). TLDs are passive dosimeters that are small, accurate and well-suited for dose verification in the routinely used 1.5 mL sample vials. For this project, three TLDs were sealed in a small plastic bag, placed into 1.5 mL tubes containing 900 μ L dH₂O, were placed horizontally and submerged under 1.3 cm dH₂O, and irradiated as described in ‘Generalized Linac irradiation protocol’. After the vials were irradiated, the TLDs were read out in the University of Wisconsin Medical Radiation Research center (UWMRRC) TLD lab and compared to the calculated dose. Non-irradiated control TLDs were read out simultaneously to account for any background radiation. The TLDs were calibrated with a separate ⁶⁰Co beam in the University of Wisconsin Accredited Dosimetry Calibration Laboratory (UWADCL), which provides independent National Institute of Standards and Technology (NIST) traceability for the measurements. This serves as an independent check of the ion-chamber based dose calculation method used to determine the beam-on time for this project. The estimated overall uncertainty on the TLD measured values is +/-5% with a coverage factor of k=1.

Generalized Linac irradiation protocol

Samples were maintained at 4 °C and transported to the University of Wisconsin Medical Radiation Research Center (UWMRRC) Varian 21EX clinical linear accelerator (Linac) facility for irradiation. The total transport time was approximately 15 min to and from the Linac facility. For each irradiation, the Linac was set to deliver a beam of electrons with 6 MeV of energy to uniformly irradiate all samples (a total of 14) at once. To accomplish this, a special high-dose mode called HDTSe⁻ was utilized, which resulted in a dose rate to the samples of approximately 72 Gy/min. The sample tubes were placed horizontally and submerged at a depth of 1.3 cm (measured to the center of the tube's volume) in an ice-water filled plastic tank and set to a source-to-surface distance (SSD) of 61.7 cm. A 30 x 30 cm² square field size was set at the Linac console, which gave an effective field size at this SSD of 18.5 x 18.5 cm². This is ample coverage to provide a uniform dose to all of the sample vials. The monitor unit calculations (determination of the amount of time to leave the Linac on) were based on the American Association of Physicists in Medicine (AAPM) Task Group 51 protocol for reference dosimetry (89). This is the standard method for determining dose per monitor unit in water for radiation therapy calculations. Once the dose was determined in the AAPM Task Group 51 reference protocol conditions (SSD = 100 cm and depth = 10 cm), an ion chamber and water-equivalent plastic slabs were used to translate this dose to the specific conditions used in this project

Linac photon mode

The Linac is designed to deliver dose with either electron or photon beams. In photon mode, the electron beam first strikes a flattening filter (not present in electron mode) to produce bremsstrahlung photons and also flatten the beam intensity profile. In order to rule out any

effective differences between electron and photon modes during irradiations, the sample vials were irradiated with the same dose rates for both modes by altering the source-to-surface-distance (SSD) for each mode.

Ionizing radiation resistance assay using the Linac

Strains were grown in biological triplicate overnight and to an OD₆₀₀ of approximately 0.2 in LB as routinely performed. A 1 mL sample for each dose tested (including 0 Gy) was removed and aliquoted into a sterile 1.5 mL microfuge tube. Samples were pelleted by centrifugation at 13 xg for 1 min, and the supernatant was poured off. Samples were resuspended in 1 mL ice-cold 1X phosphate-buffered saline (PBS), and pelleting was repeated. This process was repeated three more times to wash cells. A 100µL aliquot of each culture was removed, serial diluted 1:10 in 900µL of PBS to a final 10,000-fold dilution and 100µL was plated on LB agar to determine the colony forming units (CFU)/mL before irradiation. Samples were maintained at 4 °C and irradiated with the appropriate doses as described. A 100µL aliquot of each culture was removed and plated to determine CFU/mL and percent survival as described.

Directed evolution protocol using Linac

For each round of directed evolution, separate aliquots of 2 mL of LB medium was inoculated with frozen stock of each population from the previous round of selection. These were incubated overnight with aeration at 37 °C and were grown with usual practices in LB medium to an OD₆₀₀ of 0.2 the next day. Each culture was incubated on ice for 10 minutes to stop growth. Three 1 mL samples were removed and aliquoted into sterile 1.5 mL microfuge tubes. Samples were washed three times with 1 mL ice-cold 1X phosphate-buffered saline (PBS) and

resuspended in a final volume of 1 mL of 1X PBS. A 100 μ L aliquot of each culture was removed, serial diluted 1:10 in 900 μ L of PBS to a final 10,000-fold dilution and 100 μ L was plated on LB agar to determine the colony forming units (CFU)/mL before irradiation. Samples were maintained at 4 °C and taken to a Varian 21EX clinical linear accelerator (Linac) for irradiation.

After irradiation, an aliquot of each culture was removed, serial diluted 1:10 in 900 μ L of PBS to a final 1,000-fold dilution, and 100 μ L of each serial dilution was plated on LB agar for each dose to determine the CFU/mL after irradiation. LB agar plates were incubated overnight at 37 °C. Remaining irradiated cultures pelleted by centrifugation at 13 xg and supernatant was discarded. These pellets were resuspended in 1 mL of fresh LB medium, and this was added to 1 mL LB medium in a 5 mL glass culture tube. These resuspensions were incubated overnight with aeration at 37 °C. The following day, the percent survival for each dose was calculated using CFU/mL calculations before and after irradiation at each dose. The overnight culture of each population replicate showing closest to 1% survival was stored at -80 °C and used for the next cycle of selection. One cycle of selection was performed weekly due to limited access to the Linac.

The initiating round of selection was done as described above, except the original culture used was an overnight culture of MG1655 prepared from an isolated colony. This protocol was adapted from a previously used protocol (1).

UV Resistance Assay

Cells from a single colony of each strain were cultured overnight and then grown to an OD₆₀₀ of ~ 0.2 as in *Growth conditions*. Samples were diluted and spotted onto 25 mL 1.5% LB

agar described in the *Serial dilutions*. Spots were dried before the plate lid was removed and spots were exposed to the appropriate dose of UV irradiation using a Spectrolinker XL-1000 UV Crosslinker (Spectronics Corporation, Westbury, NY). Plates were imaged after incubation for 24 hr.

Resistance to DNA-damaging agents

Cells were grown overnight and to an OD₆₀₀ of approximately 0.2 in LB as routinely performed. Samples were mixed by vortexing for 5 s and were serially diluted 1:10 in 900 µl phosphate-buffered saline (PBS) to a final 100,000-fold dilution. Ten µl was removed from each dilution and spotted onto 30 mL 1.5% LB agar medium supplemented with 10 or 7.5 ng/ml ciprofloxacin hydrochloride as specified, 0.5 µM bleomycin, 4 µg/mL mitomycin C, or 5 mM hydroxyurea. Spots were dried before being incubated overnight at 37 °C. Plates were imaged after 48 hr for ciprofloxacin and bleomycin plates.

Growth Competition Assay

This assay was adapted from a previously published protocol (2, 48). To differentiate strains within the competition, a fitness-neutral deletion of the *araBAD* operon was introduced into one of the two strains. This deletion results in red colonies on tetrazolium arabinose (TA) agar plates (48). Briefly, overnight culture of each strain to be competed were mixed 1:1, or 1:9 (for growth competitions using isolates from the evolved populations after round 50 of selection or RpoB or ArcB mutations, in favor of the losing competitor) in a 1.5 mL tube. Samples were mixed by vortexing for 5 s and were serially diluted 1:10 in 900 µl phosphate-buffered saline (PBS) to a final dilution of 1:100,000. One hundred µL of the final dilution was spread plated

onto TA agar plates to assay for CFU. Seventy μ l of the remaining cell mixture was used to inoculate 5 mL of fresh LB media for growth overnight. This overnight culture was used to inoculate fresh media the following day, and 100 μ l was serially diluted and plated as noted above. This procedure was repeated twice more over a period of two days. The number of white versus red CFU was noted after each day of the competition and the total percentage of the culture for each competitor was determined.

Deep Sequencing

Genomic DNA was prepped from overnight cultures prepared from frozen stocks of populations from every even round of selection using the Wizard Genomic DNA Purification Kit (Promega, Madison, WI). DNA samples were submitted to the Department of Energy Joint Genome Institute (Walnut Creek, CA) for sequencing and analysis. DNA was randomly sheared into ~500bp fragments and the resulting fragments were used to create an Illumina library. This library was sequenced on Illumina HiSeq generating 100bp paired end reads. Reads were aligned to the reference genome using BWA (90), downsampled to an average depth of 250 fold coverage with picard (<http://broadinstitute.github.io/picard>) and putative mutations and small indels were called using callvariants.sh from BBMap (sourceforge.net/projects/bbmap).

Sequencing results are reported in their entirety in Supplemental Data 1 through 4. However, for analysis of numbers and types of mutations in each population (and consequently for generating Fig. 8, and Table 1 through 3), mutations in genes with high homology throughout the genome (as in *rrs*, *rrl*, *rrn*, *rhs*, and *ins* genes) were not considered due to increased likelihood of a false-positive mutation call. In addition, mutations with inconsistent frequency

calls (ex: jumping from 0, to 100, to 0% allele frequency) were also not used. All mutations removed from consideration are also listed in Supplemental Data 1 through 4.

Growth Curves

Strains were cultured described as in *Growth conditions* overnight and to an OD₆₀₀ of 0.2 in LB medium, EZ medium supplemented with 0.2% glucose (Teknova; Hollister, CA) and M9 minimal medium (85) supplemented with 0.2% glucose. Cultures were then diluted 1:100 in the appropriate medium in a clear, flat bottom 96-well plate (Fisher product #: 07-200-656) and incubated overnight in a Biotek Synergy 2 plate reader (Biotek; Winooski, VT) at 37 °C with shaking, with OD₆₀₀ readings taken by the plate reader every 10 minutes.

Acknowledgements

This work was supported by grant GM112757 from the National Institute of General Medical Sciences (NIGMS), and by grants 2817 and 502930 from the Joint Genome Institute, United States Department of Energy. Steven Bruckbauer was supported by a Morgridge Biotechnology Scholarship from the Vice Chancellor's Office for Research and Graduate Education, University of Wisconsin-Madison. Joseph Trimarco was supported by the Hilldale Undergraduate Fellowship (UW – Madison).

References

1. Harris DR, Pollock SV, Wood EA, Goiffon RJ, Klingele AJ, Cabot EL, Schackwitz W, Martin J, Eggington J, Durfee TJ, Middle CM, Norton JE, Popelars M, Li H, Klugman SA, Hamilton LL, Bane LB, Pennacchio L, Albert TJ, Perna NT, Cox MM, Battista JR.

2009. Directed evolution of radiation resistance in *Escherichia coli*. J Bacteriol 191:5240-5252.
2. Byrne RT, Klingele AJ, Cabot EL, Schackwitz WS, Martin JA, Martin J, Wang Z, Wood EA, Pennacchio C, Pennacchio LA, Perna NT, Battista JR, Cox MM. 2014. Evolution of extreme resistance to ionizing radiation via genetic adaptation of DNA repair. eLife 3:e01322.
3. Daly MJ. 2012. Death by protein damage in irradiated cells. DNA Repair 11:12-21.
4. Cox MM, Battista JR. 2005. *Deinococcus radiodurans* - The consummate survivor. Nat Rev Microbiol 3:882-892.
5. Tanaka M, Earl AM, Howell HA, Park MJ, Eisen JA, Peterson SN, Battista JR. 2004. Analysis of *Deinococcus radiodurans*'s transcriptional response to ionizing radiation and desiccation reveals novel proteins that contribute to extreme radioresistance. Genetics 168:21-33.
6. Fredrickson JK, Li SM, Gaidamakova EK, Matrosova VY, Zhai M, Sulloway HM, Scholten JC, Brown MG, Balkwill DL, Daly MJ. 2008. Protein oxidation: key to bacterial desiccation resistance? Isme J 2:393-403.
7. Battista JR, Earl AM, Park MJ. 1999. Why is *Deinococcus radiodurans* so resistant to ionizing radiation? Trends Microbiol 7:362-5.
8. Rainey FA, Ray K, Ferreira M, Gatz BZ, Nobre MF, Bagaley D, Rash BA, Park MJ, Earl AM, Shank NC, Small AM, Henk MC, Battista JR, Kampfer P, da Costa MS. 2005. Extensive diversity of ionizing-radiation-resistant bacteria recovered from Sonoran desert soil and description of nine new species of the genus *Deinococcus* obtained from a single soil sample. Appl Environ Microbiology 71:5225-5235.

- 732 9. Rainey FA, Nobre MF, Schumann P, Stackebrandt E, Dacosta MS. 1997. Phylogenetic
733 diversity of the *Deinococci* as determined by 16s ribosomal DNA sequence comparison.
734 Int J Syst Bacteriol 47:510-514.
- 735 10. Daly MJ, Gaidamakova EK, Matrosova VY, Kiang JG, Fukumoto R, Lee DY, Wehr NB,
736 Viteri GA, Berlett BS, Levine RL. 2010. Small-molecule antioxidant proteome-shields in
737 *Deinococcus radiodurans*. PLoS One 5:e12570.
- 738 11. Daly MJ, Gaidamakova EK, Matrosova VY, Vasilenko A, Zhai M, Venkateswaran A,
739 Hess M, Omelchenko MV, Kostandarithes HM, Makarova KS, Wackett LP, Fredrickson
740 JK, Ghosal D. 2004. Accumulation of Mn(II) in, *Deinococcus radiodurans* facilitates
741 gamma-radiation resistance. Science 306:1025-1028.
- 742 12. Slade D, Radman M. 2011. Oxidative Stress Resistance in *Deinococcus radiodurans*.
743 Microbiol Mol Biol Rev 75:133-191.
- 744 13. Selvam K, Duncan JR, Tanaka M, Battista JR. 2013. DdrA, DdrD, and PprA:
745 components of UV and mitomycin C resistance in *Deinococcus radiodurans* R1. PLoS
746 One 8:e69007.
- 747 14. Earl AM, Mohundro MM, Mian IS, Battista JR. 2002. The IrrE protein of *Deinococcus*
748 *radiodurans* R1 is a novel regulator of *recA* expression. J Bacteriol 184:6216-24.
- 749 15. Harris DR, Tanaka M, Saveliev SV, Jolivet E, Earl AM, Cox MM, Battista JR. 2004.
750 Preserving genome integrity: The DdrA protein of *Deinococcus radiodurans* R1. PLoS
751 Biol 2:e304.
- 752 16. Witkin EM. 1946. Inherited differences in sensitivity to radiation in *Escherichia coli*.
753 Proc Natl Acad Sci USA 32:59-68.

- 754 17. Parisi A, Antoine AD. 1974. Increased radiation resistance of vegetative *Bacillus*
755 *pumilus*. Appl Microbiol 28:41-6.
- 756 18. Davies R, Sinskey AJ. 1973. Radiation-resistant mutants of *Salmonella typhimurium*
757 LT2: development and characterization. J Bacteriol 113:133-44.
- 758 19. Erdman IE, Thatcher FS, Macqueen KF. 1961. Studies on the irradiation of
759 microorganisms in relation to food preservation. II. Irradiation resistant mutants. Can J
760 Microbiol 7:207-15.
- 761 20. Chou HH, Chiu HC, Delaney NF, Segre D, Marx CJ. 2011. Diminishing returns epistasis
762 among beneficial mutations decelerates adaptation. Science 332:1190-1192.
- 763 21. Cooper TF, Rozen DE, Lenski RE. 2003. Parallel changes in gene expression after
764 20,000 generations of evolution in *Escherichia coli*. Proc Natl Acad Sci USA 100:1072-
765 1077.
- 766 22. Good BH, McDonald MJ, Barrick JE, Lenski RE, Desai MM. 2017. The dynamics of
767 molecular evolution over 60,000 generations. Nature 551:45-50.
- 768 23. Lieberman TD, Michel JB, Aingaran M, Potter-Bynoe G, Roux D, Davis MR, Skurnik D,
769 Leiby N, LiPuma JJ, Goldberg JB, McAdam AJ, Priebe GP, Kishony R. 2011. Parallel
770 bacterial evolution within multiple patients identifies candidate pathogenicity genes. Nat
771 Genet 43:1275-1280.
- 772 24. Tenaillon O, Barrick JE, Ribeck N, Deatherage DE, Blanchard JL, Dasgupta A, Wu GC,
773 Wielgoss S, Cruveiller S, Medigue C, Schneider D, Lenski RE. 2016. Tempo and mode
774 of genome evolution in a 50,000-generation experiment. Nature 536:165-170.

- 775 25. Wannier TM, Kunjapur AM, Rice DP, McDonald MJ, Desai MM, Church GM. 2018.
776 Adaptive evolution of genomically recoded *Escherichia coli*. Proc Natl Acad Sci USA
777 115:3090-3095.
- 778 26. Woods R, Schneider D, Winkworth CL, Riley MA, Lenski RE. 2006. Tests of parallel
779 molecular evolution in a long-term experiment with *Escherichia coli*. Proc Natl Acad Sci
780 USA 103:9107-9112.
- 781 27. Luksza M, Lassig M. 2014. A predictive fitness model for influenza. Nature 507:57-61.
- 782 28. Miller CR, Joyce P, Wichman HA. 2011. Mutational effects and population dynamics
783 during viral adaptation challenge current models. Genetics 187:185-202.
- 784 29. Miller CR, Nagel AC, Scott L, Settles M, Joyce P, Wichman HA. 2016. Love the one
785 you're with: replicate viral adaptations converge on the same phenotypic change. PeerJ
786 4:e2227.
- 787 30. Morris DH, Gostic KM, Pompei S, Bedford T, Luksza M, Neher RA, Grenfell BT, Lassig
788 M, McCauley JW. 2018. Predictive modeling of influenza shows the promise of applied
789 evolutionary biology. Trends Microbiol 26:102-118.
- 790 31. Zanini F, Brodin J, Thebo L, Lanz C, Bratt G, Albert J, Neher RA. 2015. Population
791 genomics of inpatient HIV-1 evolution. eLife 4:e11282.
- 792 32. Kvitek DJ, Sherlock G. 2013. Whole genome, whole population sequencing reveals that
793 loss of signaling networks is the major adaptive strategy in a constant environment. PLoS
794 Genet 9:e1003972.
- 795 33. Lang GI, Rice DP, Hickman MJ, Sodergren E, Weinstock GM, Botstein D, Desai MM.
796 2013. Pervasive genetic hitchhiking and clonal interference in forty evolving yeast
797 populations. Nature 500:571-574.

- 798 34. Alexandrov LB, Nik-Zainal S, Wedge DC, Aparicio S, Behjati S, Biankin AV, Bignell
799 GR, Bolli N, Borg A, Borresen-Dale AL, Boyault S, Burkhardt B, Butler AP, Caldas C,
800 Davies HR, Desmedt C, Eils R, Eyfjord JE, Foekens JA, Greaves M, Hosoda F, Hutter B,
801 Ilicic T, Imbeaud S, Imielinski M, Jager N, Jones DTW, Jones D, Knappskog S, Kool M,
802 Lakhani SR, Lopez-Otin C, Martin S, Munshi NC, Nakamura H, Northcott PA, Pajic M,
803 Papaemmanuil E, Paradiso A, Pearson JV, Puente XS, Raine K, Ramakrishna M,
804 Richardson AL, Richter J, Rosenstiel P, Schlesner M, Schumacher TN, Span PN, Teague
805 JW, Totoki Y., Tutt A. N. J., Valdes-Mas, R., van Buuren, M. M., van 't Veer, L.,
806 Vincent-Salomon, A., Waddell, N., Yates, L. R., Zucman-Rossi, J., Futreal, P. A.,
807 McDermott, U., Lichter, P., Meyerson, M., Grimmond, S. M., Siebert, R., Campo, E.,
808 Shibata, T., Pfister, S. M., Campbell, P. J., Stratton, M. R., Australian Pancreatic Canc,
809 Genome, IcgC Breast Canc Consortium, IcgC Mmml- Seq Consortium, IcgC PedBrain.
810 2013. Signatures of mutational processes in human cancer. *Nature* 500:415-421.
- 811 35. Alexandrov LB, Jones PH, Wedge DC, Sale JE, Campbell PJ, Nik-Zainal S, Stratton MR.
812 2015. Clock-like mutational processes in human somatic cells. *Nat Genet* 47:1402-1407.
- 813 36. Alexandrov LB, Ju YS, Haase K, Van Loo P, Martincorena I, Nik-Zainal S, Totoki Y,
814 Fujimoto A, Nakagawa H, Shibata T, Campbell PJ, Vineis P, Phillips DH, Stratton MR.
815 2016. Mutational signatures associated with tobacco smoking in human cancer. *Science*
816 354:618-622.
- 817 37. Bolli N, Avet-Loiseau H, Wedge DC, Van Loo P, Alexandrov LB, Martincorena I,
818 Dawson KJ, Iorio F, Nik-Zainal S, Bignell GR, Hinton JW, Li YL, Tubio JMC, McLaren
819 S, Meara SO, Butler AP, Teague JW, Mudie L, Anderson E, Rashid N, Tai YT, Shammas
820 MA, Sperling AS, Fulciniti M, Richardson PG, Parmigiani G, Magrangeas F, Minvielle

S, Moreau P, Attal M, Facon T, Futreal PA, Anderson KC, Campbell PJ, Munshi NC. 2014. Heterogeneity of genomic evolution and mutational profiles in multiple myeloma. *Nat Commun* 5:2997.

38. Gundem G, Van Loo P, Kremeyer B, Alexandrov LB, Tubio JMC, Papaemmanuil E, Brewer DS, Kallio HML, Hoegnas G, Annala M, Kivinummi K, Goody V, Latimer C, O'Meara S, Dawson KJ, Isaacs W, Emmert-Buck MR, Nykter M, Foster C, Kote-Jarai Z, Easton D, Whitaker HC, Neal DE, Cooper CS, Eeles RA, Visakorpi T, Campbell PJ, McDermott U, Wedge DC, Bova GS, Grp IPU. 2015. The evolutionary history of lethal metastatic prostate cancer. *Nature* 520:353-357.

39. Hunter KW, Amin R, Deasy S, Ha NH, Wakefield L. 2018. Genetic insights into the morass of metastatic heterogeneity. *Nat Rev Cancer* 18:211-223.

40. Kandoth C, McLellan MD, Vandin F, Ye K, Niu BF, Lu C, Xie MC, Zhang QY, McMichael JF, Wyczalkowski MA, Leiserson MDM, Miller CA, Welch JS, Walter MJ, Wendl MC, Ley TJ, Wilson RK, Raphael BJ, Ding L. 2013. Mutational landscape and significance across 12 major cancer types. *Nature* 502:333-339.

41. Martincorena I, Campbell PJ. 2015. Somatic mutation in cancer and normal cells. *Science* 349:1483-1489.

42. Morganella S, Alexandrov LB, Glodzik D, Zou XQ, Davies H, Staaf J, Sieuwerts AM, Brinkman AB, Martin S, Ramakrishna M, Butler A, Kim HY, Borg A, Sotiriou C, Futreal PA, Campbell PJ, Span PN, Van Laere S, Lakhani SR, Eyfjord JE, Thompson AM, Stunnenberg HG, de Vijver MJV, Martens JWM, Borresen-Dale AL, Richardson AL, Kong G, Thomas G, Sale J, Rada C, Stratton MR, Birney E, Nik-Zainal S. 2016. The topography of mutational processes in breast cancer genomes. *Nature Commun* 7:11383.

- 844 43. Nik-Zainal S, Van Loo P, Wedge DC, Alexandrov LB, Greenman CD, Lau KW, Raine
845 K, Jones D, Marshall J, Ramakrishna M, Shlien A, Cooke SL, Hinton J, Menzies A,
846 Stebbings LA, Leroy C, Jia MM, Rance R, Mudie LJ, Gamble SJ, Stephens PJ, McLaren
847 S, Tarpey PS, Papaemmanuil E, Davies HR, Varela I, McBride DJ, Bignell GR, Leung K,
848 Butler AP, Teague JW, Martin S, Jonsson G, Mariani O, Boyault S, Miron P, Fatima A,
849 Langerod A, Aparicio S, Tutt A, Sieuwerts AM, Borg A, Thomas G, Salomon AV,
850 Richardson AL, Borresen-Dale AL, Futreal PA, Stratton MR, Campbell PJ, Int Canc
851 Genome C. 2012. The life history of 21 breast cancers. *Cell* 149:994-1007.
- 852 44. Vogelstein B, Papadopoulos N, Velculescu VE, Zhou SB, Diaz LA, Kinzler KW. 2013.
853 Cancer genome landscapes. *Science* 339:1546-1558.
- 854 45. Wedge DC, Gundem G, Mitchell T, Woodcock DJ, Martincorena I, Ghorri M, Zamora J,
855 Butler A, Whitaker H, Kote-Jarai Z, Alexandrov LB, Van Loo P, Massie CE, Dentre S,
856 Warren AY, Verrill C, Berney DM, Dennis N, Merson S, Hawkins S, Howat W, Lu YJ,
857 Lambert A, Kay J, Kremeyer B, Karaszi K, Luxton H, Camacho N, Marsden L, Edwards
858 S, Matthews L, Bo V, Leongamornlert D, McLaren S, Ng A, Yu YW, Zhang HW,
859 Dadaev T, Thomas S, Easton DF, Ahmed M, Bancroft E, Fisher C, Livni N, Nicol D,
860 Tavaré S, Gill P, Greenman C, Khoo V, Van As N, Kumar, P., Ogden, C., Cahill, D.,
861 Thompson, A., Mayer, E., Rowe, E., Dudderidge, T., Gnanapragasam, V., Shah, N. C.,
862 Raine, K., Jones, D., Menzies, A., Stebbings, L., Teague, J., Hazell, S., Corbishley, C., de
863 Bono, J., Attard, G., Isaacs, W., Visakorpi, T., Fraser, M., Boutros, P. C., Bristow, R. G.,
864 Workman, P., Sander, C., Hamdy, F. C., Futreal, A., McDermott, U., Al-Lazikani, B.,
865 Lynch, A. G., Bova, G. S., Foster, C. S., Brewer, D. S., Neal, D. E., Cooper, C. S., Eeles,
866 R. A., Camcap Study Grp, Tcga Consortium. 2018. Sequencing of prostate cancers

867 identifies new cancer genes, routes of progression and drug targets. Nat Genet 50:682-
868 692.

869 46. Rokyta DR, Joyce P, Caudle SB, Miller C, Beisel CJ, Wichman HA. 2011. Epistasis
870 between beneficial mutations and the phenotype-to-fitness map for a ssDNA virus. PLoS
871 Genet 7:e1002075.

872 47. Bruckbauer ST, Trimarco JD, Henry C, Wood EA, Battista JR, Cox MM. 2019. A variant
873 of the *Escherichia coli* anaerobic transcription factor FNR exhibiting diminished
874 promoter activation function enhances ionizing radiation resistance. PLoS One in press.

875 48. Lenski RE, Rose MR, Simpson SC, Tadler SC. 1991. Long-term experimental evolution
876 in *Escherichia coli*. 1. Adaptation and divergence during 2,000 generations. American
877 Naturalist 138:1315-1341.

878 49. Povirk LF. 1987. Mutational specificity of bleomycin. Proc Amer Assoc Cancer Res
879 28:117-117.

880 50. Povirk LF. 1987. Bleomycin-induced base substitutions in the lambda-cI gene. Environ
881 Mutagen 9:86-86.

882 51. Hendricks SP, Mathews CK. 1998. Differential effects of hydroxyurea upon
883 deoxyribonucleoside triphosphate pools, analyzed with vaccinia virus ribonucleotide
884 reductase. J Biol Chem 273:29519-29523.

885 52. Sakano K, Oikawa S, Hasegawa K, Kawanishi S. 2001. Hydroxyurea induces site-
886 specific DNA damage via formation of hydrogen peroxide and nitric oxide. Jap J Cancer
887 Res 92:1166-1174.

888 53. Singh A, Xu YJ. 2016. The cell killing mechanisms of hydroxyurea. Genes 7:99.

- 889 54. Weinberger M, Trabold PA, Lu M, Sharma K, Huberman JA, Burhans WC. 1999.
890 Induction by adozelesin and hydroxyurea of origin recognition complex-dependent DNA
891 damage and DNA replication checkpoints in *Saccharomyces cerevisiae*. J Biol Chem
892 274:35975-35984.
- 893 55. Xie C-X, Xu A, Wu L-J, Yao J-M, Yang J-B, Yu Z-L. 2004. Comparison of base
894 substitutions in response to nitrogen ion implantation and ⁶⁰Co-gamma ray irradiation in
895 *Escherichia coli*. Genet Mol Biol 27:284-290.
- 896 56. Wang D, Kreutzer DA, Essigmann JM. 1998. Mutagenicity and repair of oxidative DNA
897 damage: insights from studies using defined lesions. Mut Res-Fund Mol Mech Mutagen
898 400:99-115.
- 899 57. Elena SF, Lenski RE. 2003. Evolution experiments with microorganisms: The dynamics
900 and genetic bases of adaptation. Nature Rev Genet 4:457-469.
- 901 58. Toprak E, Veres A, Michel JB, Chait R, Hartl DL, Kishony R. 2012. Evolutionary paths
902 to antibiotic resistance under dynamically sustained drug selection. Nature Genet 44:101-
903 U140.
- 904 59. Amundsen SK, Taylor AF, Chaudhury AM, Smith GR. 1986. recD: the gene for an
905 essential third subunit of exonuclease V. Proc Natl Acad Sci USA 83:5558-62.
- 906 60. Biek DP, Cohen SN. 1986. Identification and characterization of *recD*, a gene affecting
907 plasmid maintenance and recombination in *Escherichia coli*. J Bacteriol 167:594-603.
- 908 61. Chaudhury AM, Smith GR. 1984. A new class of *Escherichia coli* *recBC* mutants -
909 implications for the role of RecBC enzyme in homologous recombination. Proc Natl
910 Acad Sci USA 81:7850-7854.

- 911 62. Thaler DS, Sampson E, Siddiqi I, Rosenberg SM, Thomason LC, Stahl FW, Stahl MM.
912 1989. Recombination of bacteriophage lambda in recD mutants of *Escherichia coli*.
913 Genome 31:53-67.
- 914 63. Uranga LA, Reyes ED, Patidar PL, Redman LN, Lusetti SL. 2017. The cohesin-like
915 RecN protein stimulates RecA-mediated recombinational repair of DNA double-strand
916 breaks. Nature Commun 8:15282.
- 917 64. Wang G, Maier RJ. 2008. Critical role of RecN in recombinational DNA repair and
918 survival of *Helicobacter pylori*. Infect Immun 76:153-160.
- 919 65. Picksley SM, Morton SJ, Lloyd RG. 1985. The *recN* locus of *Escherichia coli* K12:
920 molecular analysis and identification of the gene product. Mol Gen Genet 201:301-7.
- 921 66. Meddows TR, Savory AP, Grove JJ, Moore T, Lloyd RG. 2005. RecN protein and
922 transcription factor DksA combine to promote faithful recombinational repair of DNA
923 double-strand breaks. Mol Microbiol 57:97-110.
- 924 67. Brena-Valle M, Serment-Guerrero J. 1998. SOS induction by gamma-radiation in
925 *Escherichia coli* strains defective in repair and/or recombination mechanisms. Mutagen
926 13:637-641.
- 927 68. Cashel M, Gentry DR, Hernandez VJ, Vinella D. 1996. The Stringent Response, p 1458-
928 1495. In Neidhardt FC, Curtiss RI (ed), *Escherichia coli* and *Salmonella*: Cell Mol Biol,
929 vol 1. ASM Press, Washington, D. C.
- 930 69. Trautinger BW, Lloyd RG. 2002. Modulation of DNA repair by mutations flanking the
931 DNA channel through RNA polymerase. EMBO J 21:6944-6953.
- 932 70. McGlynn P, Lloyd RG. 2000. Modulation of RNA polymerase by (p)ppGpp reveals a
933 RecG-dependent mechanism for replication fork progression. Cell 101:35-45.

- 934 71. Epshtein V, Kamarthapu V, McGary K, Svetlov V, Ueberheide B, Proshkin S, Mironov
935 A, Nudler E. 2014. UvrD facilitates DNA repair by pulling RNA polymerase backwards.
936 Nature 505:372-377.
- 937 72. Landick R, Stewart J, Lee DN. 1990. Amino acid changes in conserved regions of the
938 beta subunit of *Escherichia coli* RNA polymerase alter transcription pausing and
939 termination. Genes Develop 4:1623-1636.
- 940 73. Barrick JE, Kauth MR, Strelisoff CC, Lenski RE. 2010. *Escherichia coli* rpoB Mutants
941 Have Increased Evolvability in Proportion to Their Fitness Defects. Mol Biol Evol
942 27:1338-1347.
- 943 74. Severinov K, Soushko M, Goldfarb A, Nikiforov V. 1993. Rifampicin region revisited -
944 new rifampicin-resistant and streptolydigin-resistant mutants in the beta subunit of
945 *Escherichia coli* RNA polymerase. J Biol Chem 268:14820-14825.
- 946 75. Zhou YN, Lubkowska L, Hui M, Court C, Chen S, Court DL, Strathern J, Jin DJ,
947 Kashlev M. 2013. Isolation and characterization of RNA Polymerase *rpoB* mutations that
948 alter transcription slippage during elongation in *Escherichia coli*. J Biol Chem 288:2700-
949 2710.
- 950 76. Deatherage DE, Kepner JL, Bennett AF, Lenski RE, Barrick JE. 2017. Specificity of
951 genome evolution in experimental populations of *Escherichia coli* evolved at different
952 temperatures. Proc Natl Acad Sci USA 114:E1904-E1912.
- 953 77. Tenaillon O, Rodriguez-Verdugo A, Gaut RL, McDonald P, Bennett AF, Long AD, Gaut
954 BS. 2012. The molecular diversity of adaptive convergence. Science 335:457-461.
- 955 78. Avrani S, Bolotin E, Katz S, Hershberg R. 2017. Rapid genetic adaptation during the first
956 four months of survival under resource exhaustion. Mol Biol Evol 34:1758-1769.

79. Conrad TM, Frazier M, Joyce AR, Cho BK, Knight EM, Lewis NE, Landick R, Palsson BO. 2010. RNA polymerase mutants found through adaptive evolution reprogram *Escherichia coli* for optimal growth in minimal media. *Proc Natl Acad Sci USA* 107:20500-20505.
80. Harden MM, He A, Creamer K, Clark MW, Hamdallah I, Martinez KA, Kresslein RL, Bush SP, Slonczewski JL. 2015. Acid-adapted strains of *Escherichia coli* K-12 obtained by experimental evolution. *Appl Environ Microbiol* 81:1932-1941.
81. He A, Penix SR, Basting PJ, Griffith JM, Creamer KE, Camperchioli D, Clark MW, Gonzales AS, Erazo JSC, George NS, Bhagwat AA, Slonczewski JL. 2017. Acid evolution of *Escherichia coli* K-12 eliminates amino acid decarboxylases and reregulates catabolism. *Appl Environ Microbiol* 83:UNSP e00442-17.
82. Mehta P, Casjens S, Krishnaswamy S. 2004. Analysis of the lambdoid prophage element e14 in the *E. coli* K-12 genome. *BMC Microbiol* 4:4.
83. Charusanti P, Conrad TM, Knight EM, Venkataraman K, Fong NL, Xie B, Gao YA, Palsson BO. 2010. Genetic basis of growth adaptation of *Escherichia coli* after deletion of *pgi*, a major metabolic gene. *PLoS Genet* 6:e1001186.
84. Wang X, Kim Y, Ma Q, Hong SH, Pokusaeva K, Sturino JM, Wood TK. 2010. Cryptic prophages help bacteria cope with adverse environments. *Nat Commun* 1:147.
85. Miller JH. 1992. A Short Course in Bacterial Genetics: A Laboratory Manual and Handbook for *Escherichia coli* and Related Bacteria. Cold Spring Harbor Laboratory, Cold Spring Harbor, NY.
86. Lenski RE. 1991. Quantifying fitness and gene stability in microorganisms. *Biotech* 15:173-92.

- 980 87. Warming S, Costantino N, Court DL, Jenkins NA, Copeland NG. 2005. Simple and
981 highly efficient BAC recombineering using galK selection. *Nuc Acids Res* 33:e36.
- 982 88. Datsenko KA, Wanner BL. 2000. One-step inactivation of chromosomal genes in
983 *Escherichia coli* K-12 using PCR products. *Proc Natl Acad Sci USA* 97:6640-6645.
- 984 89. Almond PR, Biggs PJ, Coursey BM, Hanson WF, Huq MS, Nath R, Rogers DWO. 1999.
985 AAPM's TG-51 protocol for clinical reference dosimetry of high-energy photon and
986 electron beams. *Med Phys* 26:1847-1870.
- 987 90. Li H, Durbin R. 2009. Fast and accurate short read alignment with Burrows-Wheeler
988 transform. *Bioinform* 25:1754-1760.

989

990

Figure Legends

Fig. 1. Cell killing with electron beam versus photon beam ionizing radiation. Early exponential phase cultures of MG1655 were exposed to electron beam or photon beam IR as described in the Materials and Methods. Percent survival was determined via CFU/mL counts pre- and post-irradiation. Results are representative of a single experiment performed in biological triplicate.

Fig. 2. Directed evolution scheme and lineage nomenclature. (A) *Scheme*. Briefly, overnight cultures were grown from a freezer stock of the parent strain/the evolved population from the previous round of selection. This overnight culture was used to inoculate fresh LB rich medium and cultures were grown to early exponential phase. These cultures were then separated into multiple aliquots and washed 3X in 1X PBS to remove LB medium. One aliquot of each population was irradiated with the same dose that killed 99% of the population in the previous round of selection, and the remaining aliquots were irradiated with higher doses. A portion of the irradiated aliquots were plated to determine percent survival, while the remaining culture was resuspended in fresh LB medium. These were then grown overnight, and the culture that was nearest to 1% survival (as determined by CFU counts from pre- and post-irradiation cultures) was stored at -80° C. One round of selection was conducted weekly due to limited access to the Linac. (B) *Nomenclature*. We have generated four lineages of highly IR-resistant *E. coli*, designated IR9, IR10, IR11, and IR12. A designated round of selection indicates a population at that round (Ex: IR9-50 is lineage IR9 after 50 rounds of selection). Each population has been stored at -80 °C as a ‘fossil record’ of evolution. Clonal isolates generated by streak plating a

population then streak plating ten separate isolated colonies are designated by a numeral value added to the parent population nomenclature (Ex: The first isolate from IR9-50 is IR9-50-1).

Fig. 3. Documentation of increased IR resistance. (A) *Increase in dose required to kill 99% of cells.* Each data point indicates the dose of IR that each population was given prior to being outgrown overnight (Step 6 in Fig. 2) and stored at -80° C. (Step 7 in Fig. 2). The percent survival was estimated from a single replicate at each round of selection. (B) *Survival curves of evolved populations compared to previously evolved Escherichia coli isolates and Deinococcus radiodurans.* Early exponential phase cultures of the indicated strains were exposed to electron beam IR as described in the Materials and Methods. CB2000 and CB3000 are isolates from *E. coli* populations evolved to withstand γ -ray IR (1, 2). Error bars represent the standard deviation of CFU/mL calculations from a single experiment performed in biological triplicate.

Fig. 4. Growth curves of evolved isolates in rich and minimal medium. (A) *Growth curves of isolates in LB rich medium.* (B) *Growth curves of isolates in EZ defined rich medium supplemented with 0.2% glucose.* (C) *Growth curves of isolates in M9 defined minimal medium supplemented with 0.2% glucose.* Cultures of indicated strains were grown in the appropriate medium overnight and then to early exponential phase as described in the Materials and Methods. All cultures were incubated at 37 °C during growth. Early exponential phase cultures were diluted 1:100 in the appropriate medium, and then incubated overnight in a Biotek Synergy 2 plate reader, with OD₆₀₀ measurements taken automatically every 5 minutes. Each growth curve is a representative replicate from an experiment performed in biological triplicate.

Fig. 5. Growth competitions of evolved isolates. (A) *Growth competition of IR9-50-1 against Founder Δel4.* (B) *Growth competition of IR10-50-1 against Founder Δel4.* (C) *Growth competition of IR11-50-1 against Founder Δel4.* (D) *Growth competition of IR12-50-1 against Founder Δel4.* Growth competitions were performed as described in the Materials and Methods. Briefly, competitions were started with an excess of the evolved isolate so that competitions could be carried out to 72 hr (at approximately a 9:1 ratio of evolved isolate to Founder Δel4). Even with an excess of IR9-50-1, this isolate was outcompeted by 48 hr. Deleting the *araBAD* operon causes a red colony phenotype with no fitness cost that allows for differentiation of the two strains in competition on TA medium. IR11-50-1 is red on TA medium without alteration of the *araBAD* operon, so this competition was performed against Founder Δel4 *araBAD*⁺. Error bars represent the standard deviation of CFU/mL calculations of an experiment performed in biological triplicate. Results shown are representative of two independent experiments.

Fig. 6. Evolved isolates exhibit variable survival of UV irradiation. Five isolates from each population were grown in LB medium overnight and then to early exponential phase as described in the Materials and Methods. Cultures were serially diluted in 1X PBS, and then 10 μL of each dilution was spot plated onto LB agar. Once spots dried, plates were exposed to UV irradiation and were then incubated overnight before imaging. Results shown are representative of two independent experiments performed.

Fig. 7. Evolved isolates exhibit variable survival of various DNA damaging agents. Five isolates from each population were grown in LB medium overnight and then to early exponential phase as described in the Materials and Methods. Cultures were serially diluted in 1X PBS, and

then 10 μ L of each dilution was spot plated onto LB agar with the indicated DNA-damaging agent. Once spots dried the plates were then incubated overnight before imaging. Results shown are representative of two independent experiments performed.

Fig. 8. Mutations in evolving populations. (A-D) Allele frequencies as a function of selection

round. Panels A-D reflect the indicated population, IR9, IR10, IR11, and IR12, respectively.

Whole populations at each even round of selection were deep-sequenced by the Joint Genome

Institute (JGI) as described in the *Materials and Methods*. Every mutation that reached at least

2% frequency at some point in a single population are depicted as single lines. The sole black

line in each graph represents the loss of the ϕ 14 prophage. Mutations that reach a frequency of

“1.00” are fixed, and subsequent mutations occur within that genetic background. The y-axis

represents the allele frequency of each single mutation within the population (i.e. a mutation at

0.5 is in 50% of the isolates in the population). The x-axis represents the round of selection.

Allele frequency data was generated from every even cycle of selection. Graphs were generated

using the R library “ggplot2”. Line colors are utilized primarily to allow ready distinctions

between subpopulations, but otherwise have no significance. Data used to generate these plots

are contained within Supplemental Data 1 through 4. **(E) Number of mutations over rounds of**

selection in evolving populations. Each data point represents the total number of detected

mutations at or above 2% frequency in each sequenced whole population. The number of

mutations generally increases, but experience dips as major sub-populations are driven to

extinction. Data used to generate this plot are contained within Supplemental Data 1 through 4.

Fig. 9. Mutations which contribute to IR resistance in the evolved isolate IR9-50-1. (A) *IR resistance of Founder Δ e14 derivatives containing mutations from lineage IR9.* Mutations were moved singly or in combination from IR9-50-1 (in the case of ArcB N405D, from IR9-20-1; the *recD* deletion was made in the Founder Δ e14 parent strain) into the Founder Δ e14 strain background as described in the Materials and Methods. A '+' symbol indicates that the variant is present in that strain. **(B)** *IR resistance of IR9-50-1 derivatives containing reversions of mutations to the wild-type sequence.* Wild-type sequences of the gene encoding the indicated protein variants was moved from Founder Δ e14 into IR9-50-1 as described in the Materials and Methods (IR9-50-1 does not have a ArcB variant, therefore no reversion was tested in this strain). A '-' symbol indicates that the variant was reverted to the wild-type allele in that strain. Each strain was assayed for IR resistance alongside biological triplicate of the parent strain (a Founder Δ e14 or IR9-50-1 control) and the average percent survival of the experimental strains was compared to that of the parent strain. All strains were exposed to 1000 Gy of electron beam IR and percent survival was determined via calculating CFU/mL before and after irradiation. Error bars represent the standard deviation of CFU/mL calculations of at least two independent experiments performed in biological triplicate. Statistical significance of percent survival relative to the parent strain was determined using a two-tailed Student's T-test. The '*' and '****' represent p-values of < 0.05 and < 0.001, respectively.

Fig. 10. Frequencies of mutations implicated in IR resistance over rounds of selection. Frequencies of mutations in genes implicated in evolved IR resistance (*rpoB*, *recA*, *recD*, *recN*) and the loss of the e14 prophage are depicted. Both synonymous and non-synonymous mutations are included. These data seemingly indicate two separate paths to acquiring IR resistance: loss of

the e14 prophage, gain of an *rpoB*, then *recD*, then *recN* mutation, in that order (IR9, IR11, IR12), or gain of a *recA* and *recD* mutation in concert (IR10). In lineages IR11 and IR12, these two pathways to IR resistance appear in direct competition, with the *rpoB*, *recD*, and *recN* path being the apparent ‘winner’. Data used to generate these plots are contained within Supplemental Data 1 through 4.

Fig. 11. Effects of prevalent mutations on growth. Two mutations from lineage IR9 have opposite effects on growth; ArcB N405D greatly enhances growth of Founder Δ e14 whereas the RpoB S72N/RpoC K1172I mutations greatly hinder growth. These results suggest that mutation not seen to affect IR resistance (ArcB N405D) may be selected for in these populations to counteract the deleterious growth effects of mutations which enhance IR resistance. Growth competition assays were performed as described in the Materials and Methods. Initial ratios of each strain were purposefully mixed at 9 (loser):1 (winner) so that growth competition assays could be carried out for longer than 24 hr. Results shown are representative of two independent experiments performed.

Tables

Table 1. Number and types of mutations in evolved populations after 50 cycles of selection.

Mutations in coding regions that likely cause loss of function of the protein product (single and double base insertions/deletions, gain or loss of stop codons, and loss of start codons) appeared in each population. However, IR9-50 had the most predicted loss of function mutations (72) compared to the other three populations (IR10-50: 48, IR11-50: 40, IR12-50: 49). Of these mutations in all populations, -1 frameshift mutations were the most common, followed by introduced stop codons.

Table 2. Mutations that are likely candidates for enhancing IR resistance. Proteins listed are encoded by genes that have i) mutations that were non-synonymous; ii) mutations that occurred in a gene that was mutated in at least two additional populations; iii) mutations that achieved at least 10% abundance at some point during selection in each population in which they appeared; and iv) the mutation remained in the population at round 50 of selection. The mutations in RecA and Nth were included as these are the only proteins with the same variant present in two populations. The bolded variants are fixed in the indicated population, the variants listed in black are present above 2% frequency at round 50 of selection, and variants listed in gray were present in the indicated lineage but have been driven extinct by round 50 of selection.

Table 3. Number of mutations in isolates from evolved populations after 50 cycles of selection. Nomenclature of the isolates indicates the lineage (ex: IR9) and round of selection (ex:50) from which the isolate was derived. The remaining numeral distinguishes the individual

1150 isolates.

1151

1152 **Table 4. List of strains used in this study.** Strains generated in this study were constructed as
1153 described in the Materials and Methods. A ‘wt’ designation indicates that the protein is variant at
1154 the indicated allele in the evolved isolate but has been swapped to the wild-type (MG1655)
1155 allele. The ‘*’ symbol indicates that this nucleotide position is in reference to the NCBI
1156 GenBank U00096.3 reference genome.

1157

1158

1159

1160 Table 1

1161		Parent bp	Mutant bp	IR9-50	IR10-50	IR11-50	IR12-50
1162	Transitions	AT	GC	93	106	94	110
		GC	AT	180	158	130	223
	Transversions	AT	CG	26	17	11	25
		GC	TA	154	116	84	143
		AT	TA	81	58	59	85
		GC	CG	41	25	31	51
	Transitions			273	264	224	333
	Transversions			302	216	185	304
	Total			575	480	409	637
	Coding	Synonymous		127	124	98	171
		Non-synonymous		340	275	237	363
		dN/dS		2.68	2.22	2.42	2.12
		Stop gained		29	15	12	16
		Stop lost		1	2	0	1
		Start lost		0	0	1	2
		Insertions	+1	1	2	2	3
			+2	0	0	0	0
			+3	0	0	1	0
			+12	0	0	1	0
		Deletions	-1	40	26	21	26
			-2	0	1	1	2
			-3	1	0	0	0
	Non-coding	SNPs		81	70	65	92
		Insertions	+1	0	0	0	0
			+2	0	0	0	1
			+3	0	0	0	0
		Deletions	-1	3	6	4	6
			-2	0	0	0	1
			-3	0	0	0	0
	Allele frequencies	Fixed (>99%)		107	84	20	76
		>50%		242	109	130	150
		>10 %		309	199	205	320
		>2%		620	515	439	676

1163 Table 2

1164

1165

Pathway	Protein	IR9	IR10	IR11	IR12
Anaerobic respiration	ArcB	N405D	D166Y S280R L90 fs Y71C	R100H S74W	S24P K547 fs
Copper metabolism	CopA	V270F		T525A	A812V
DNA metabolism	DinI	R28H P14A	W71*	I66N	S26Y
	Nth		C203Y E160K		C203Y K85N
	RecA	Y294C	A290S	A290S E286G	E19K
	RecD	A90E L188* L223* P99*	N124D Q463* L301M	A550E A39G C71 fs G307W W534R	S92I A271E C103* T568A
	RecN	K429Q E271G R118L	F144L	R102P S382R	A361T R285C R368H S310L
RNA polymerase	RpoB	S72N S391P	F15L K1200E	P535L S574F	T600I

1166 Table3

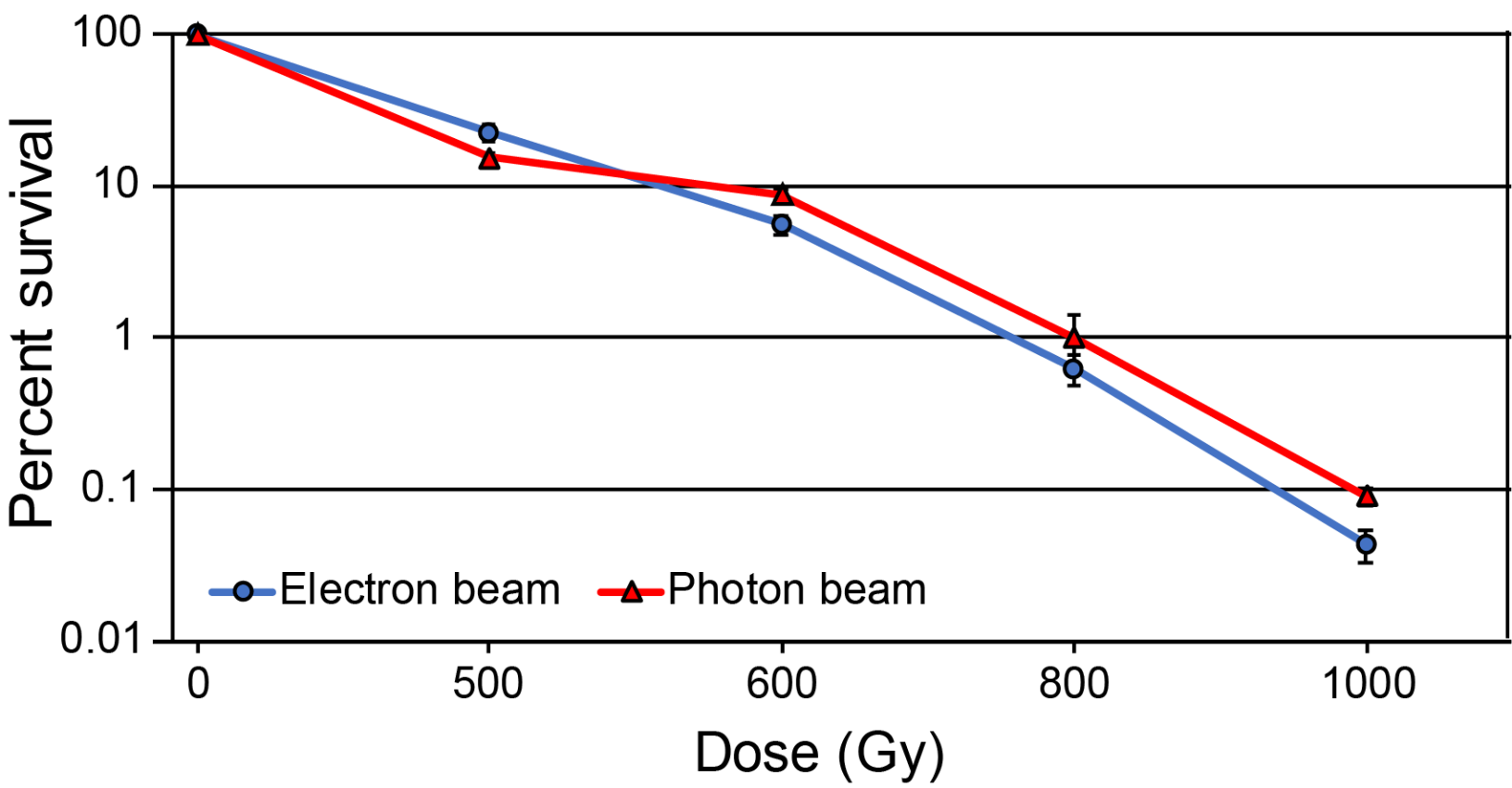
1167

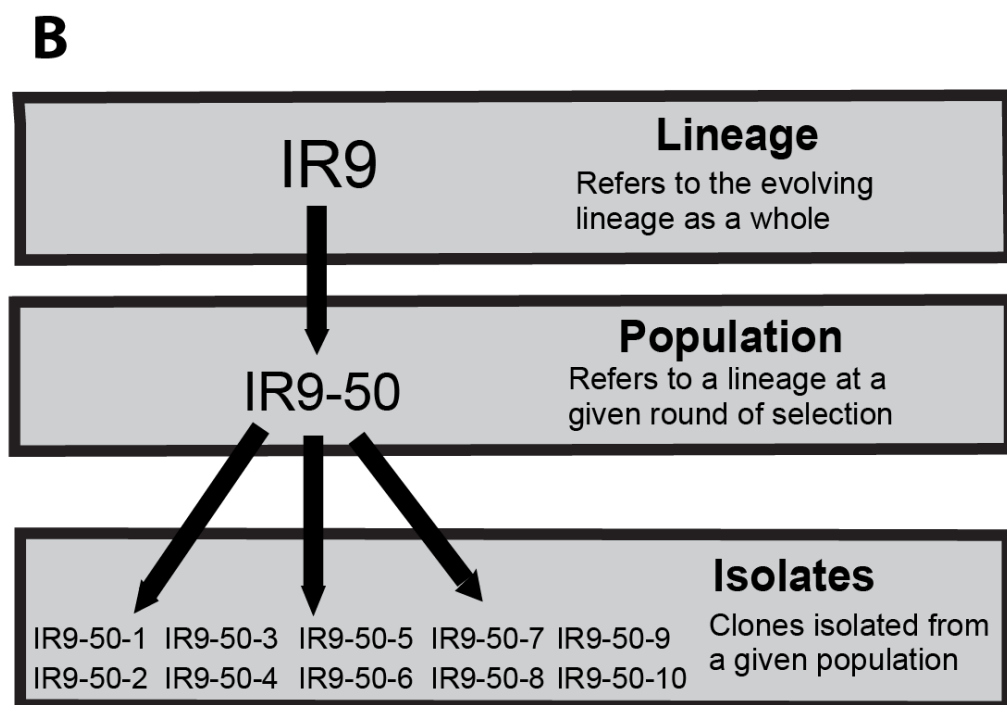
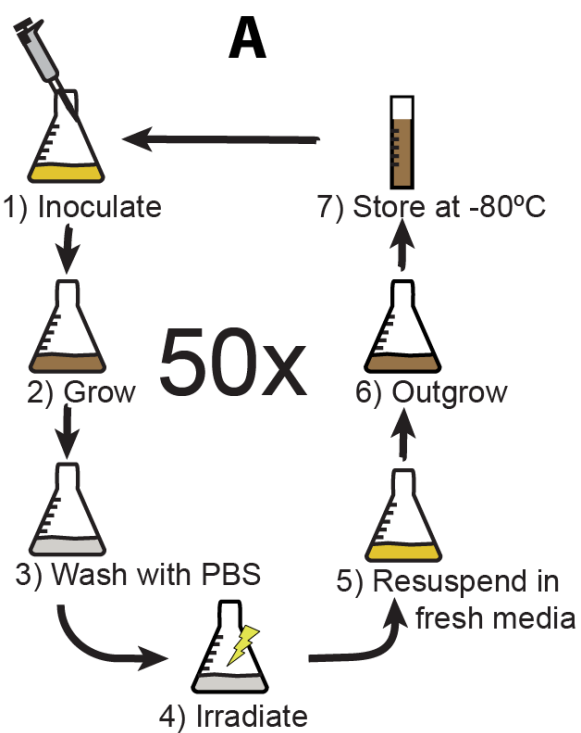
1168

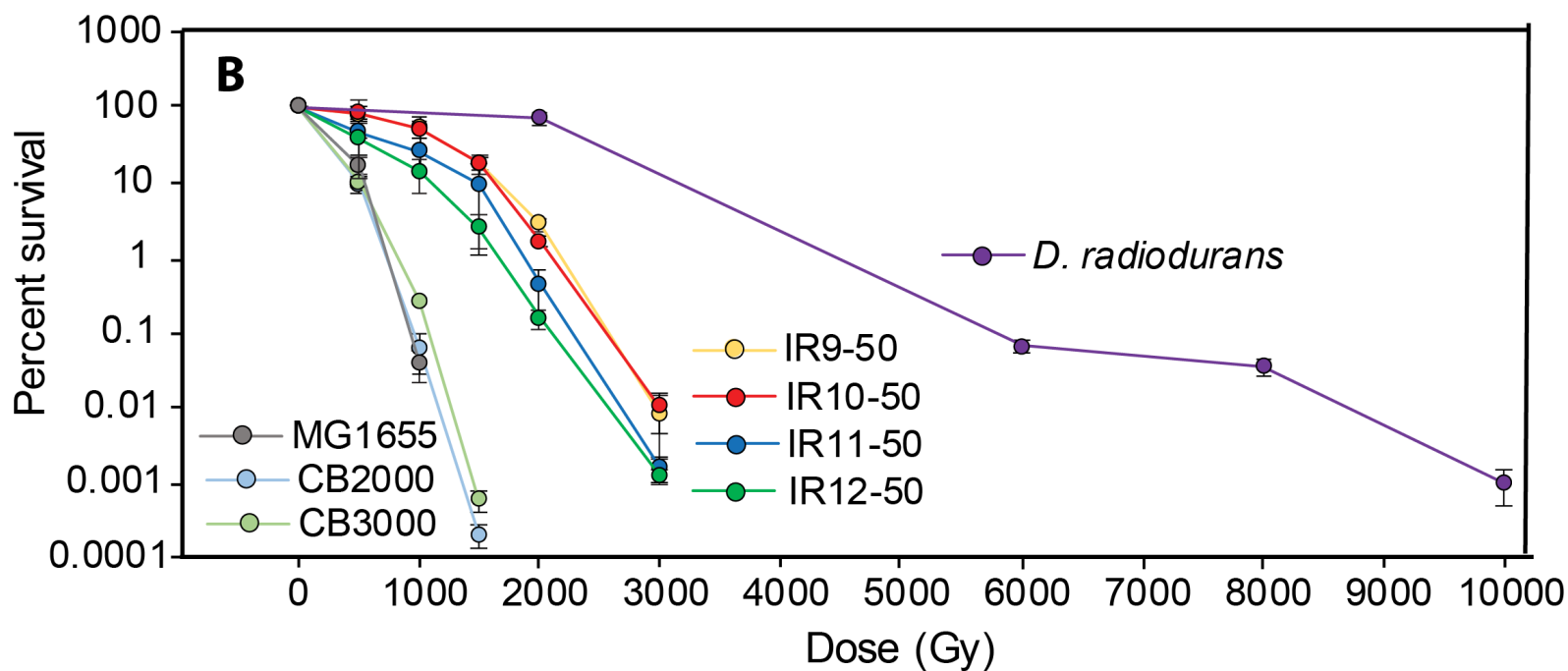
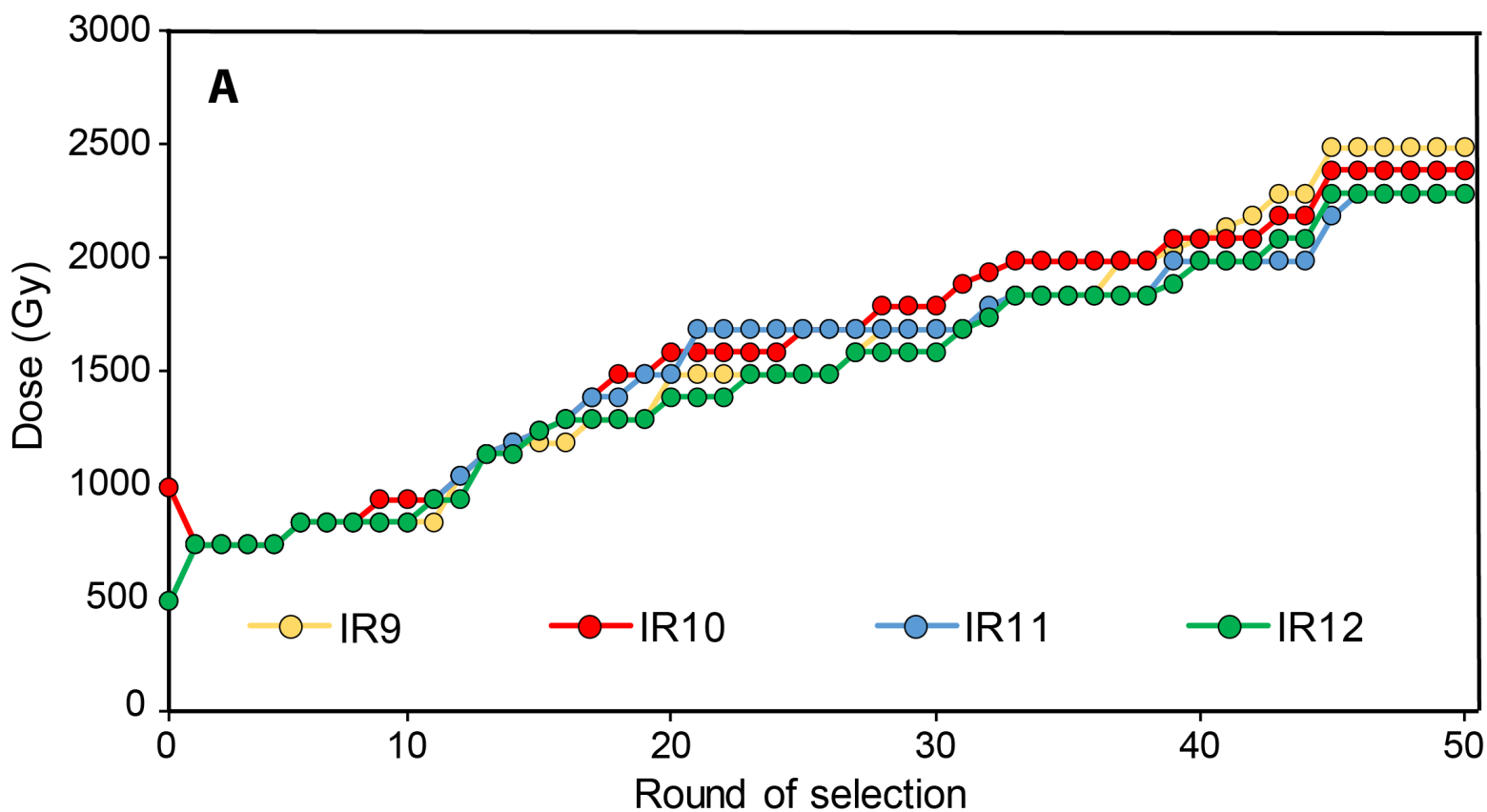
Isolate	Number of Mutations
IR9-50-1	312
IR9-50-2	298
IR9-50-3	299
IR9-50-4	314
IR9-50-5	322
IR10-50-1	184
IR10-50-2	188
IR10-50-3	197
IR10-50-4	210
IR10-50-5	191
IR11-50-1	200
IR11-50-2	192
IR11-50-3	194
IR11-50-4	182
IR11-50-5	197
IR12-50-1	280
IR12-50-2	241
IR12-50-3	245
IR12-50-4	232
IR12-50-5	237

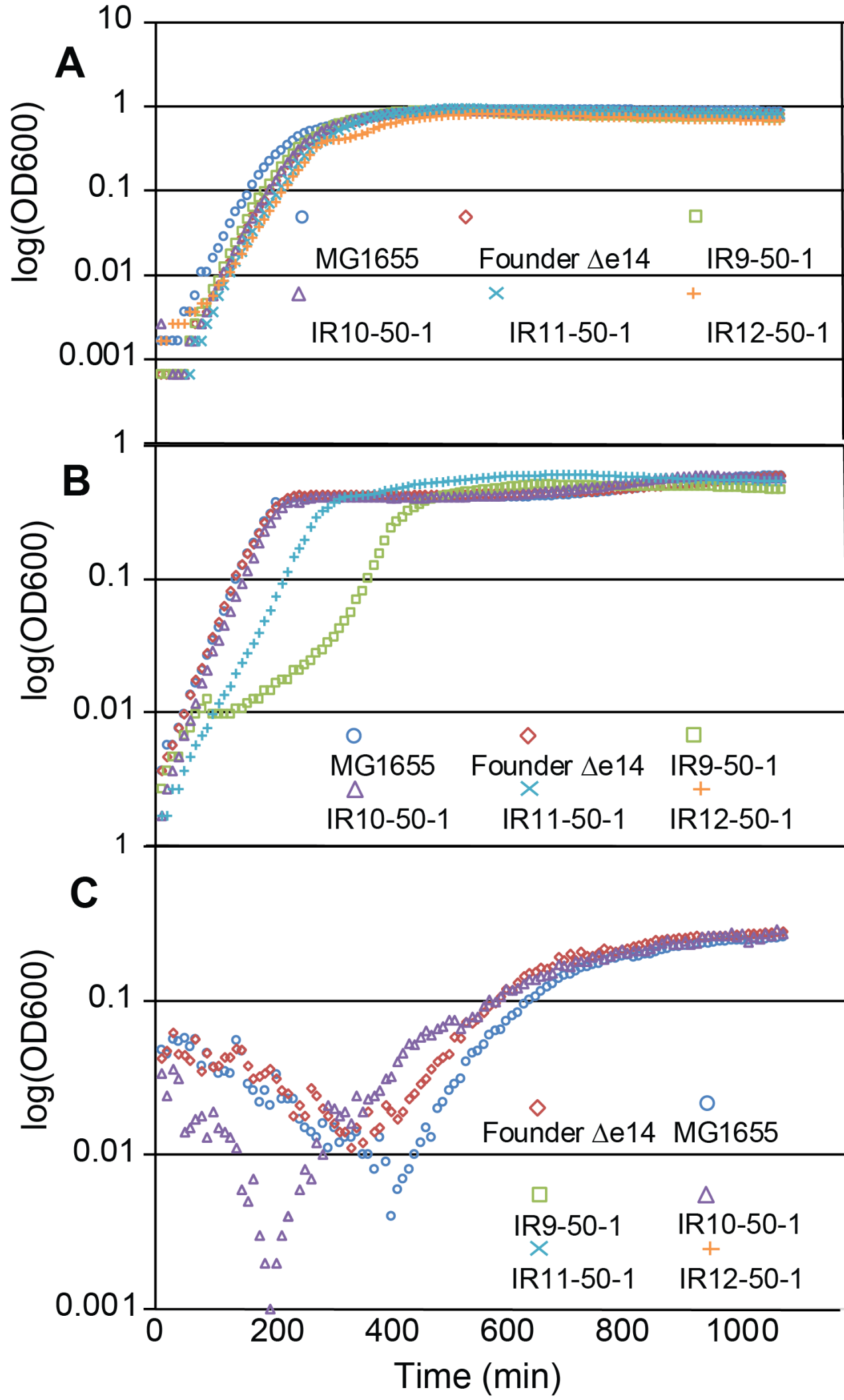
Strain	Relevant Genotype	Source
MG1655	YbhJ L54I + MntP G25D + RIP321 A 4296380* ACG + GlpR C 3560455* CG + GatC ACC 2173360* A	Blattner, 1997
EAW7704 (Founder Δe14)	MG1655 Δe14 + RbsR L92R + CytR Q110 stop + <i>fabI/ycjD</i> int (G 1351174* A) + <i>yifN/ppiC</i> int (T 3959934* C)	Harris, 2009
IR9-50	MG1655 exposed to 50 iterative rounds of IR; mixed population	This study
IR10-50	MG1655 exposed to 50 iterative rounds of IR; mixed population	This study
IR11-50	MG1655 exposed to 50 iterative rounds of IR; mixed population	This study
IR12-50	MG1655 exposed to 50 iterative rounds of IR; mixed population	This study
IR9-50-1	Isolate from IR9-50	This study
IR9-50-2	Isolate from IR9-50	This study
IR9-50-3	Isolate from IR9-50	This study
IR9-50-4	Isolate from IR9-50	This study
IR9-50-5	Isolate from IR9-50	This study
IR10-50-1	Isolate from IR10-50	This study
IR10-50-2	Isolate from IR10-50	This study
IR10-50-3	Isolate from IR10-50	This study
IR10-50-4	Isolate from IR10-50	This study
IR10-50-5	Isolate from IR10-50	This study
IR11-50-1	Isolate from IR11-50	This study
IR11-50-2	Isolate from IR11-50	This study
IR11-50-3	Isolate from IR11-50	This study
IR11-50-4	Isolate from IR11-50	This study
IR11-50-5	Isolate from IR11-50	This study
IR12-50-1	Isolate from IR12-50	This study
IR12-50-2	Isolate from IR12-50	This study
IR12-50-3	Isolate from IR12-50	This study
IR12-50-4	Isolate from IR12-50	This study
IR12-50-5	Isolate from IR12-50	This study
CB2000	Isolate from IR-resistant evolved population IR-2-20	Harris, 2009
CB3000	Isolate from IR-resistant evolved population IR-3-20	Harris, 2009
EAW792	Founder Δe14 + ArcB N405D	This study
EAW971	Founder Δe14 + CopA V270F	This study
EAW766	Founder Δe14 + DinI R28H	This study
JDT56	Founder Δe14 + RecA A290S	This study
EAW726	Founder Δe14 + RecD A90E	This study
EAW725	Founder Δe14 + RecN K429Q	This study
EAW756	Founder Δe14 + RpoB S72N/RpoC K1172I	This study
EAW748	Founder Δe14 + RecD A90E + RecN K428H	This study
EAW904	Founder Δe14 + RecD A90E + RpoB S72N/RpoC K1172I	This study
EAW781	Founder Δe14 + RecD A90E + RecN K428H + RpoB S72N/RpoC K1172I	This study
EAW972	IR9-50-1 + CopA V270 wt	This study
EAW1047	IR9-50-1 + DinI R28 wt	This study
EAW973	IR9-50-1 + RecD A90 wt	This study
EA1024	IR9-50-1 + RecN K429 wt	This study
EAW981	IR9-50-1 + RpoB S72/RpoC K1172 wt	This study
EAW1021	IR9-50-1 + RecD A90 wt + RpoB S72/RpoC K1172 wt	This study
EAW1046	IR9-50-1 + RecD A90 wt + RpoB S72/RpoC K1172 wt + RecN K429 wt	This study
STB75	Founder Δe14 ΔaraBAD	Bruckbauer, 2018

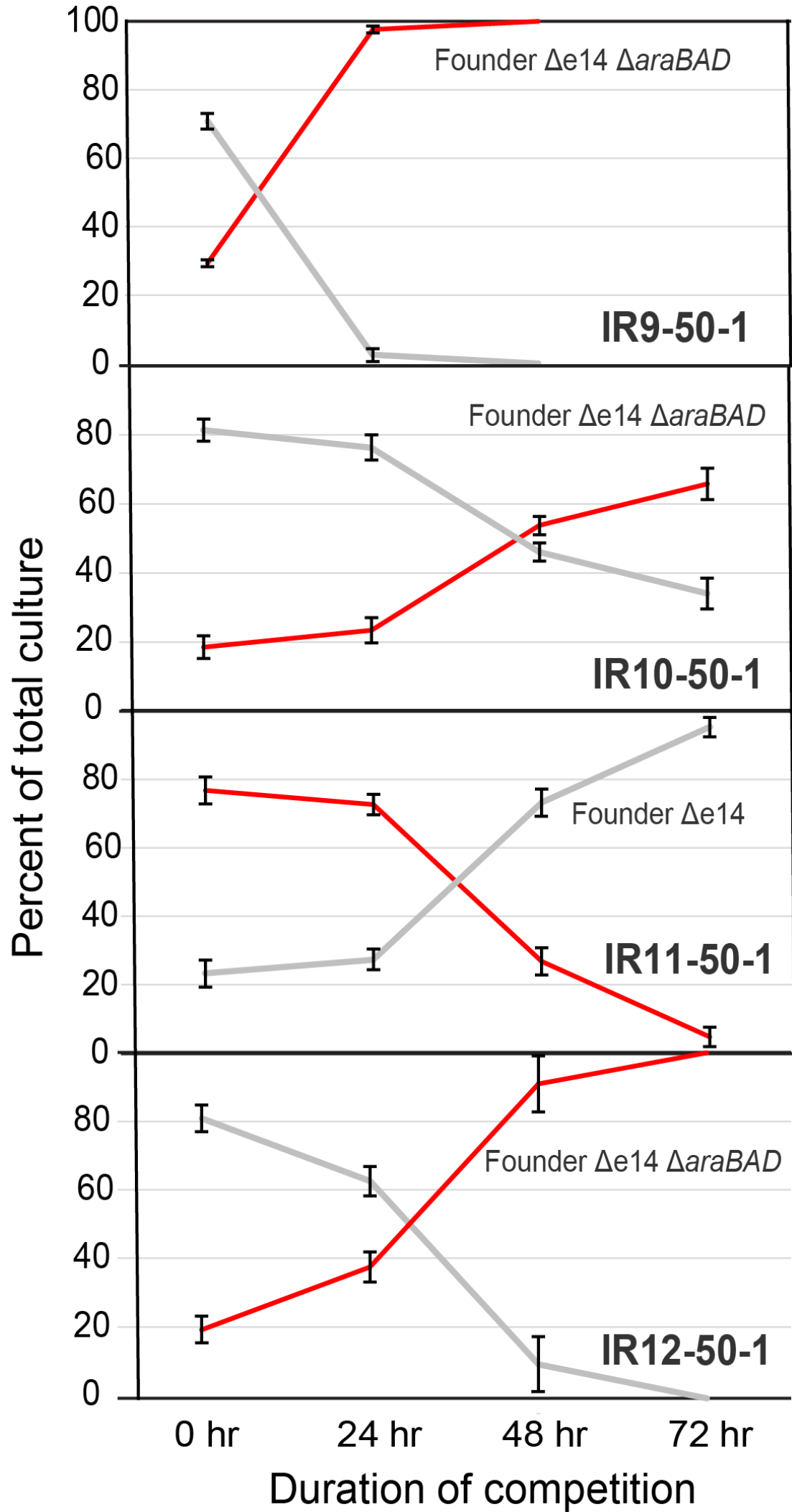
* nucleotide position compared to NCBI GenBank U00096.3 reference sequence

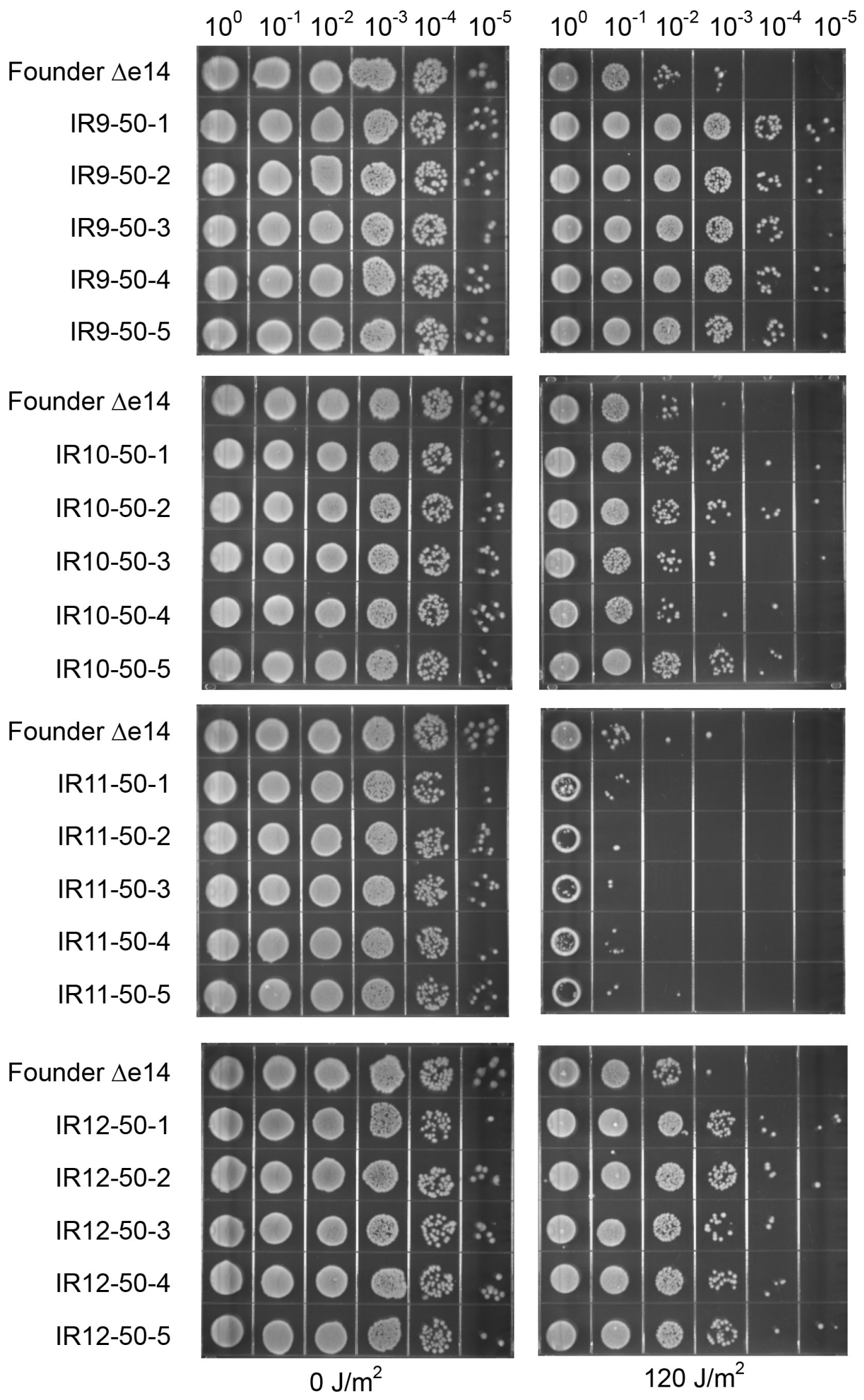


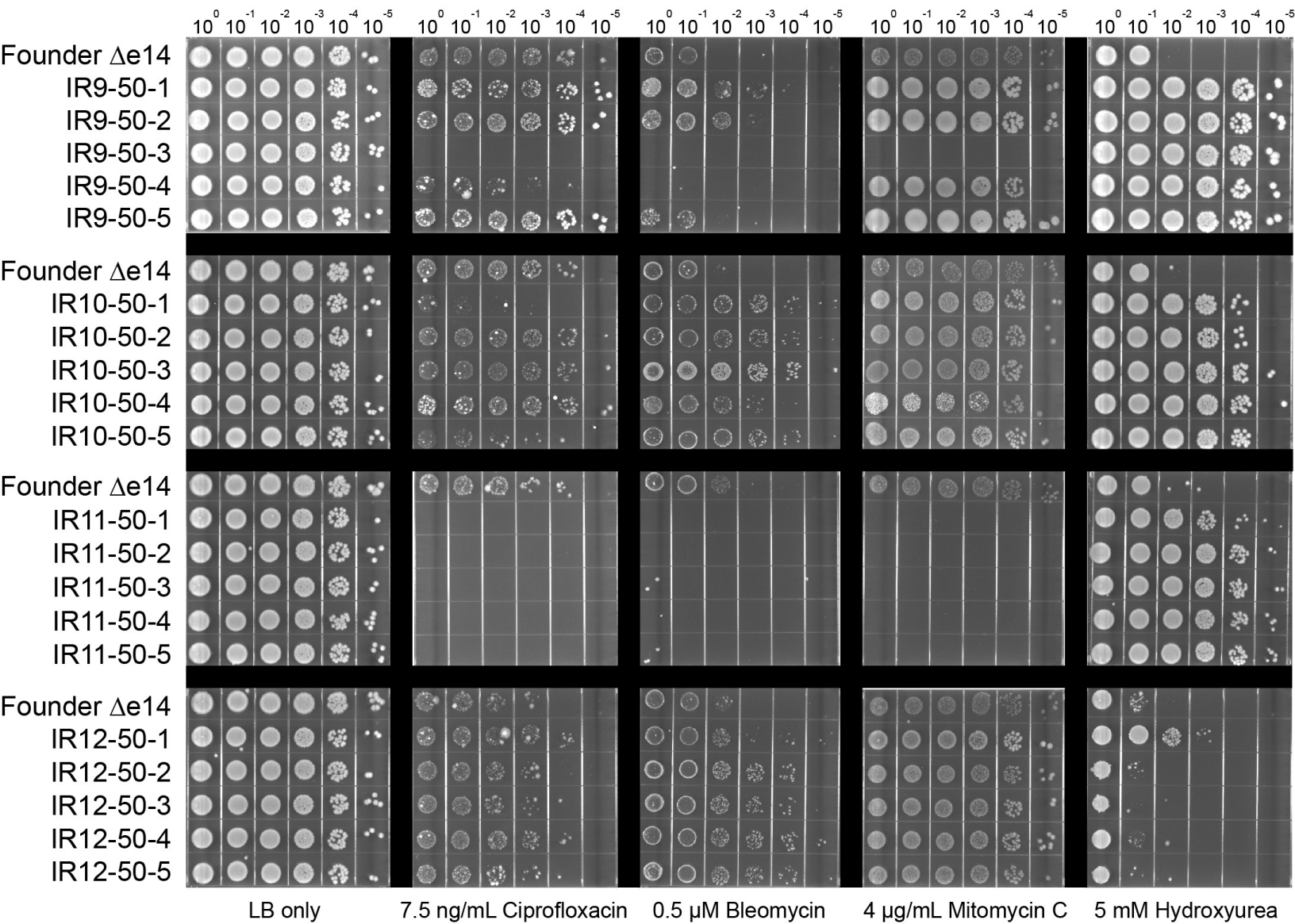


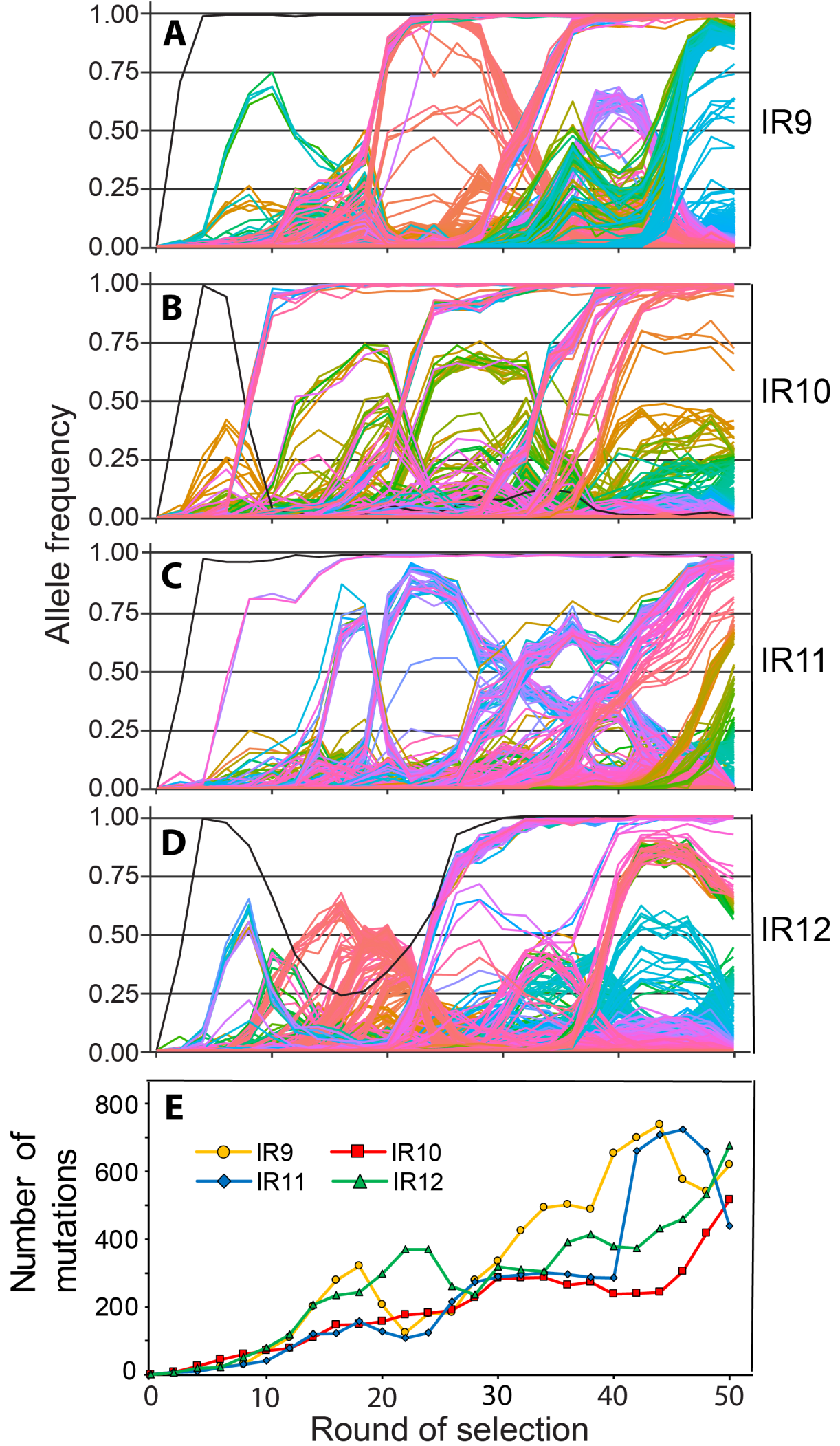






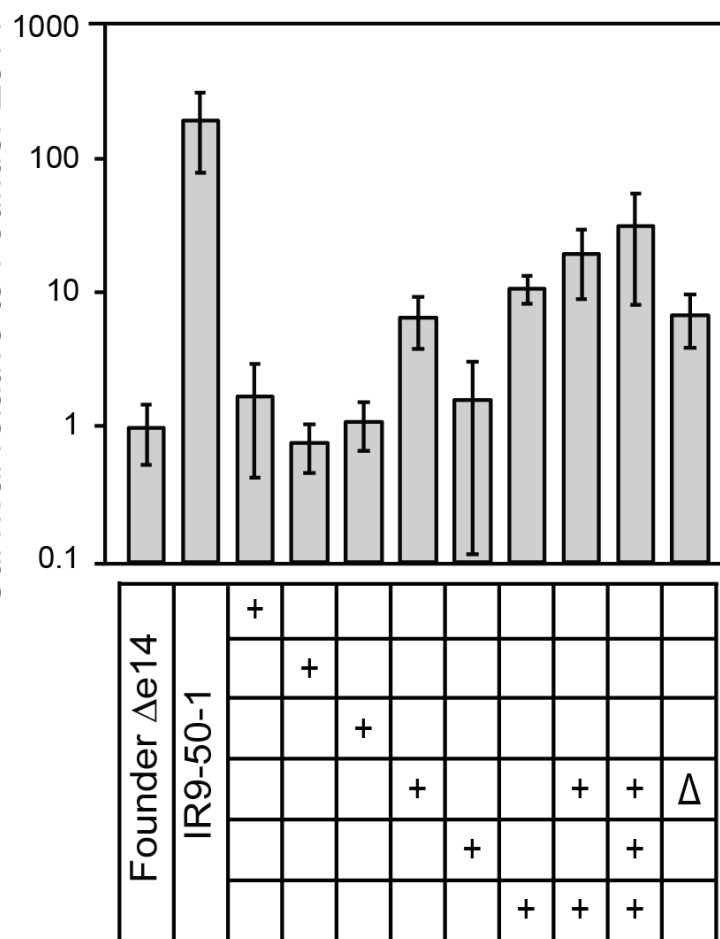




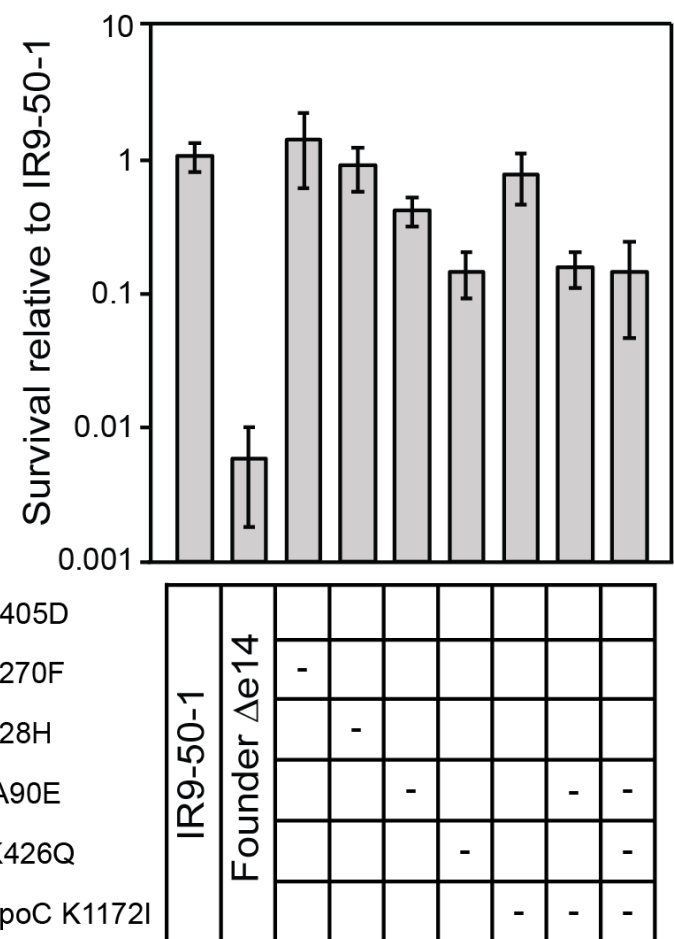


A

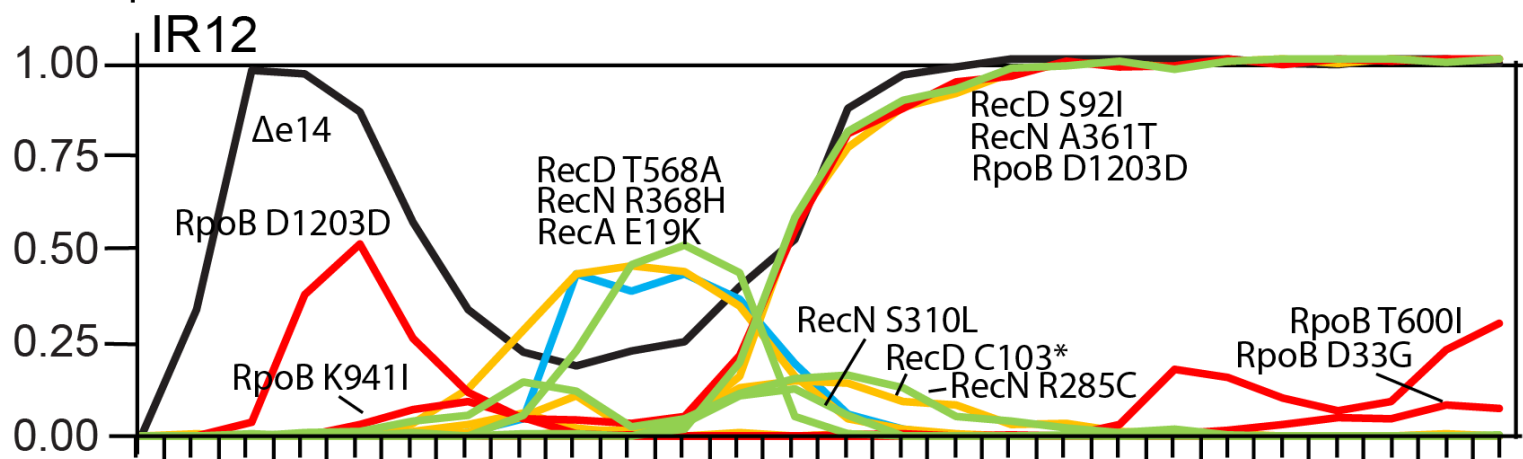
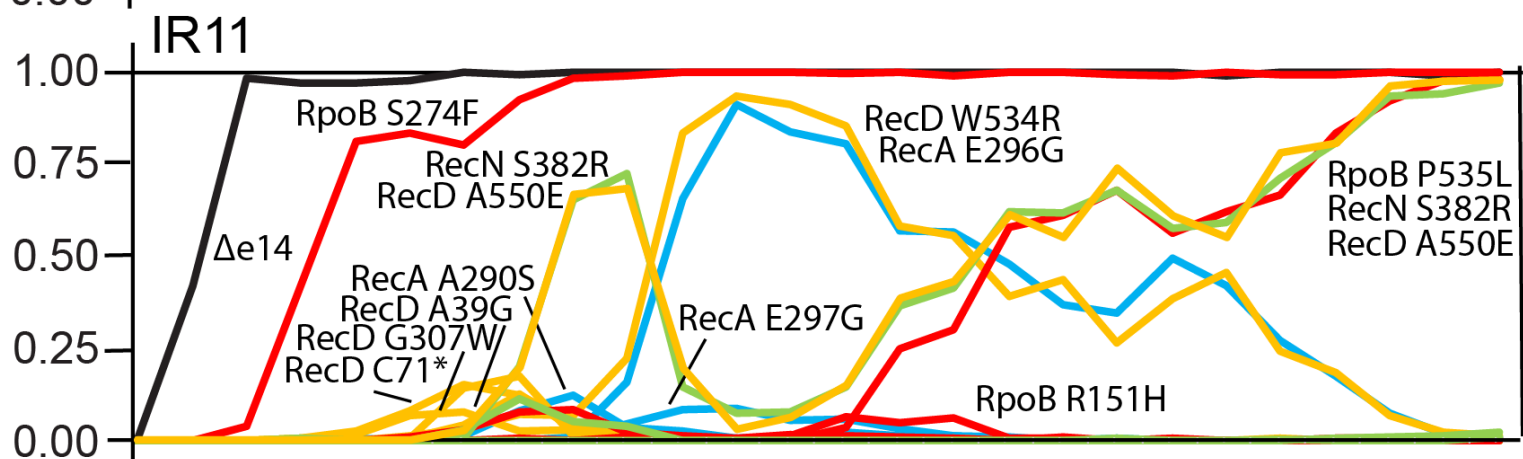
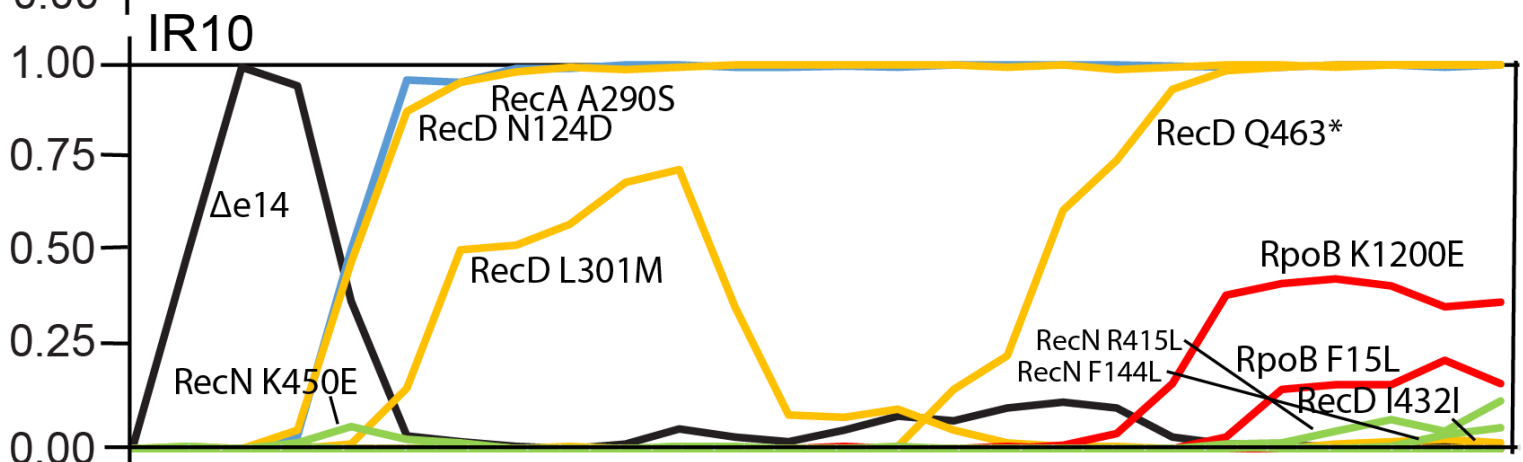
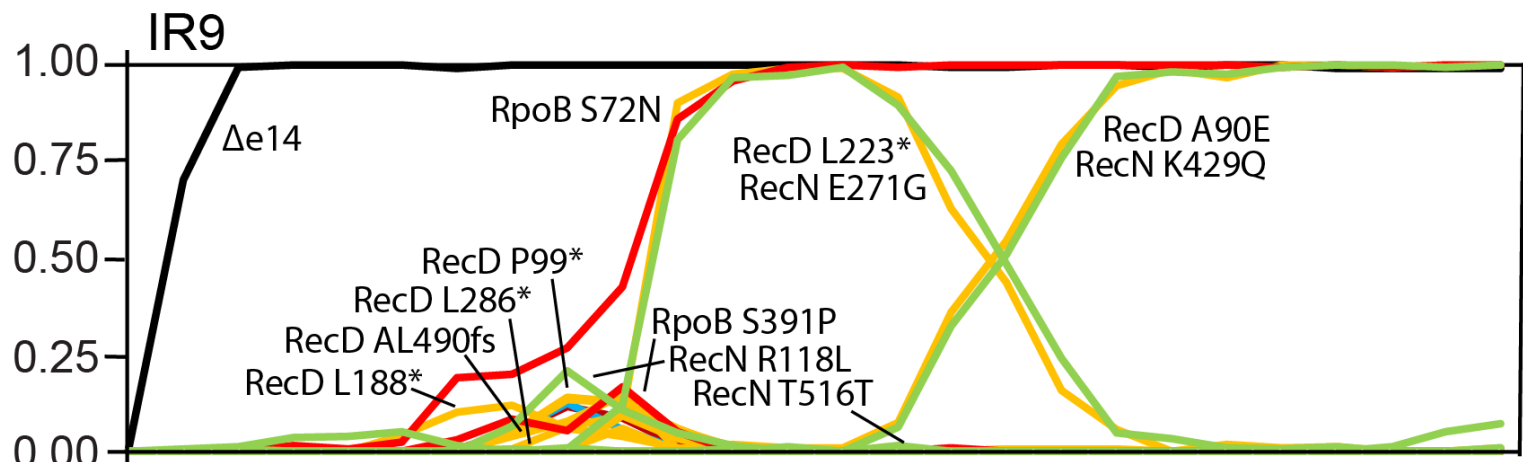
Survival relative to Founder $\Delta e14$



B



Allele frequency



0 10 20 30 40 50

Round of selection

— $\Delta e14$ — *recA* — *recD* — *recN* — *rpoB*

